SKI Report 2007:15

Research

Evaluation of the FRAPTRAN -1.3 Computer Cod

Tero Manngård

March 2007

ISSN 1104-1374
ISRN SKI-R-07/15-SE

SKI

SKI Perspective

Over the last years the behaviour of nuclear fuel during loss of coolant accidents (LOCA) has been studied to investigate the failure behaviour at high burnup and for modern fuel cladding. The results of recent experimental programmes indicate that the cladding alloy composition and high burnup effects influence LOCA acceptance criteria margins.

SKI has therefore initiated a study to investigate nuclear fuel behaviour during a LOCA. The study is divided in four parts:

- Review of experimental data and models for LWR fuel cladding behaviour under LOCA conditions.
- Critical review of FRAPTRAN-1.3 and its modelling capacity.
- Evaluation of models for cladding oxidation, embrittlement, deformation and burst under LOCA.
- Implementation of alternative models for LOCA in FRAPTRAN-1.3.

The work presented in this report is the second part of the study. In the report a review of the computer code FRAPTRAN is made and it is judge to be suitable for transient fuel rod analysis.

This project has contributed to the research goal of giving a basis for SKIs supervision by means of evaluating the computer code FRAPTRAN and its capability to model nuclear fuel cladding during a design base accident. The results are useful as such, but also are the basis for modifications to FRAPTRAN in a following project.

Responsible for the project at SKI has been Jan In de Betou.
Project Identification Number: 200606025

SKI Report 2007:15

Research

Evaluation of the FRAPTRAN -1.3 Computer Cod

Tero Manngård
Quantum Technologies AB
Uppsala Science Park
SE-751 83 Uppsala, Sweden

March 2007

This report concerns a study which has been conducted for the Swedish Nuclear Power Inspectorate (SKI). The conclusions and viewpoints presented in the report are those of the author/authors and do not necessarily coincide with those of the SKI.

List of contents

Summary

The FRAPTRAN-1.3 computer code has been evaluated regarding its applicability, modelling capability, user friendliness, source code structure and supporting experimental database. The code is intended for thermo-mechanical analyses of light water reactor nuclear fuel rods under reactor power and coolant transients, such as overpower transients, reactivity initiated accidents (RIA), boiling-water reactor power oscillations without scram, and loss of coolant accidents (LOCA). Its experimental database covers boiling- and pressurized water reactor fuel rods with UO_2 fuel up to rod burnups around 64 MWd/kgU.

In FRAPTRAN-1.3, the fundamental equations for heat transfer and structural analysis are solved in one-dimensional (in the radial direction) and transient (time-dependent) form, and interaction between axial segments of the rod is confined to calculations of coolant axial flow, rod internal gas pressure and optionally axial flow of fission gases. The clad-to-coolant heat transfer conditions can either be specified as pre-calculated data or can be determined by a coolant channel model in the code. The code provides different clad rupture models depending on cladding temperature and amount of cladding plastic hoop strain. For LOCA analysis, a model calculating local clad shape (ballooning) and associated local stresses is available to predict clad burst. A strain-based failure model is present for cladding rupture driven by pellet-cladding mechanical interaction. Two models exist for computation of high-temperature clad oxidation under LOCA (i) the Baker-Just model for licensing calculations and (ii) the Cathcart-Pawel model for best-estimate calculations.

The code appears to be fairly easy to use, however, the applicability of the current version as a self-standing analysis tool for LOCA and RIA analyses depends highly on the numerical robustness of the coolant channel model for generation of clad-to-coolant heat transfer boundary conditions.

The main documentations for FRAPTRAN are: (i) a general code description and (ii) an integral assessment report pertaining to an earlier version of the code. Correlations for materials properties (from the MATPRO package) are extensively used in the code. The material models in FRAPTRAN have been designed for Zircaloy, hence the code currently lacks support for other types cladding materials. Our evaluation shows that the code lacks capability to account for different creep rates in the α, $(\alpha+\beta)$ and β phases of cladding material as well as the phase transformation kinetics, which are necessary to discriminate the LOCA behaviour of various zirconium-based cladding materials. Suggestions for improvements of the code's applicability for LOCA analyses are pointed out in the report.

In conclusion, we believe that FRAPTRAN-1.3 constitutes a suitable computer code for transient fuel rod analysis, into which SKI can add new and improved models that satisfy their requirements.

Sammanfattning

Datorprogrammet FRAPTRAN-1.3 har utvärderats med avseende på användbarhet, modelleringsförmåga, källkodsstruktur och de experimentella data, på vilka programmets modeller är baserade. Programmet är avsett för analys av kärnbränslestavars termomekaniska beteende i lättvattenreaktorer under transienter av reaktoreffekt och kylmedel, såsom transienter med måttlig övereffekt, härdoscillationer i kokarvattenreaktorer utan framkallande av snabbstopp, reaktivitetstransienter (RIA) och olyckor orsakade av kylmedelsförlust (LOCA). Dess experimentella underlag omfattar kok- och tryckvattenreaktor bränslestavar, laddade med UO_2 bränsle, upp till 64 MWd/kgU i medelstavutbränning.

De grundläggande ekvationerna för värmetransport och stavens mekaniska beteende i FRAPTRAN-1.3 löses i endimensionell (i radiell riktning) och transient (tidsberoende) form, och koppling mellan olika axiella segment hos bränslestaven beaktas endast vid beräkning av kylmedlets axiella flöde, gastrycket inuti staven samt vid tillval vid axiellt flöde av fissionsgaser. Förhållandena för värmetransport från kapsling till kylmedel kan antingen ges som indata eller beräknas med en modell för kylmedelskanalen i programmet. I programmet finns olika modeller för kapslingsbrott, beroende på kapslingstemperatur och storlek på kapslingens plastiska töjning i tangentiell riktning. För beräkning av kapslingsbrott under LOCA används en detaljerad modell med vilken kapslingens deformationer (form) samt tillhörande lokala spänningar bestäms. För kapslingsbrott orsakad av mekanisk växelverkan mellan kutsar och kapslingsrör finns en töjningsbaserad brottmodell att tillgå. Två olika modeller finns för kvantifiering av kapslingsrörets hög-temperatur oxidation under LOCA (i) Baker-Just modellen för licensieringsberäkningar och (ii) Cathcart-Pawel modellen för ”best-estimate” (bästa uppskattning) beräkningar.

Programmet förefaller ganska lättanvänt, men användbarheten av den aktuella versionen som ett självständigt beräkningsverktyg för LOCA och RIA analyser beror i hög grad av kylkanalsmodellens förmåga (numeriska robusthet) att generera randvillkor för värmetransport vid kapslingsrörets yta.

Den huvudsakliga dokumentationen för FRAPTRAN är: (i) en allmän programbeskrivning och (ii) en övergripande utvärderingsrapport, båda rörande en tidigare version av programmet. Materialkorrelationer (från MATPRO materialdatabibliotek) används flitigt i programmet. Materialmodellerna som används in FRAPTRAN har tagits fram för Zircaloy, sålunda saknar programmet för närvarande stöd för andra typer av kapslingsmaterial. Vår utvärdering visar att programmet saknar förmåga att ta hänsyn till olika kryptöjningshastigheter i α, $(\alpha+\beta)$ och β fas hos kapslingsmaterialet liksom kinetiken vid fasomvandling, vilket är nödvändigt för att kunna skilja mellan LOCA beteende hos olika zirkonium-baserade kapslingsmaterial. Förslag på förbättringar av programmets användbarhet för LOCA analyser ges i rapporten.

Avslutningsvis anser vi att FRAPTRAN-1.3 utgör ett lämpligt beräkningsprogram för analys av bränslestavars beteende under transienta förhållanden, i vilket SKI kan införa nya och förbättrade modeller som motsvarar deras behov.

1 Introduction

This is the second report in a series of three, in which the available experimental data and models for light water reactor (LWR) fuel cladding behaviour under LOCA conditions are reviewed. The present work constitutes a critical review of the FRAPTRAN-1.3 computer code (Cunningham et al., 2001a-b; FRAPTRAN-1.3, 2005) and its modelling capability. FRAPTRAN-1.3 is intended for thermo-mechanical analysis of LWR fuel rod behaviour during reactor power and coolant transients, such as overpower transients, reactivity initiated accidents (RIA), boiling-water reactor power oscillations without scram, and loss of coolant accidents (LOCA). The fuel rod initial condition for transient analysis in FRAPTRAN-1.3 can be streamlined from any burnup step of a steady-state FRAPCON-3 (Berna et al., 1997) output (by using an initialization file). Based on the rod state, prescribed power history and coolant behaviour as a function of time, the code calculates the resulting variation with time of fuel rod temperature, deformation, internal gas pressure and optionally also cladding high-temperature oxidation behaviour, Cunningham et al. (2001a). Similar to FRAPCON-3, the FRAPTRAN code was developed for the United States Nuclear Regulatory Commission (NRC) by the Idaho National Engineering and Environmental Laboratory (INEEL) and Pacific Northwest National Laboratory (PNNL).

FRAPTRAN-1.3 is a descendent of FRAP-T6, a transient fuel rod code for thermal-mechanical analysis with ancestors in the 1970s. Since PNNL began work on FRAPTRAN in 1997, the aim has been to extend its high burnup capability and to simplify the code.

FRAPTRAN-1.3 has been assessed and validated with respect to experimental data from LOCA and RIA tests. The LOCA database used for the assessment comprises 7 unirradiated fuel rods and that for RIA 15 rodlets with fuel burnups ranging from 26 to 64 MWd/kgU.

FRAPTRAN-1.3 is linked with a subset of the MATPRO material properties package, Allison et al. (1993)[1]. Certain models that have been modified relative to MATPRO are discussed in Geelhood et al. (2004) and in the release document, FRAPTRAN-1.3 (2005).

The FRAPTRAN-1.3 code is one-dimensional in nature (in the radial direction), and interaction between axial segments of the rod is confined to calculations of coolant axial flow and rod internal gas pressure. The one-dimensional nature of the code is a significant drawback in analyses of pellet-cladding mechanical interaction, but makes the applied computational methods fairly simple and the code transparent. Moreover, the one-dimensional formulation brings down the execution times to a minimum. They are typically in the order of several minutes on the present office-class personal computers for the assessment cases provided along with the FRAPTRAN-1.3 code. However, the execution time is also much dependent on the case sophistication.

[1] MATPRO version available for FRAPCON-3/FRAPTRAN users, at www.pnl.gov/frapcon3, at time of the present FRAPTRAN-1.3 review.

The report is organized as follows:

In section 2, the FRAPTRAN-1.3 models and methods used for calculation of thermo-mechanical response, cladding high-temperature oxidation and failure are briefly reviewed. Section 3 presents an overview of input and output data to the code, and section 4 deals with code structure, implementation and documentation. Section 5 finally presents the database used for code assessment, and section 6 summarizes the most important items from the hitherto performed code review.

2 FRAPTRAN-1.3 models

The FRAPTRAN-1.3 code is intended for analyses of light water reactor (LWR) fuel rod behaviour, when power and/or coolant boundary conditions change rapidly. More specifically, it has been developed to calculate the fuel rod response under operational transients and hypothetical accidents. The code calculates the transient variation of many important fuel rod variables, such as fuel and clad temperatures, clad stresses and strains, high-temperature oxidation (optionally) and rod internal gas pressure. In addition, the code applies models for prediction of clad rupture. Burnup-dependent initial conditions generated by FRAPCON-3 can be straightforwardly imported for transient fuel rod analysis in the FRAPTRAN code. The FRAPCON-3 code has been reviewed earlier by Jernkvist & Massih (2002).

In the following, a brief summary of the general modelling capabilities and inherent limitations of the code is first presented. The summary is then followed by a more thorough evaluation of the models which are critical to its capacity for calculation of fuel rod behaviour under LOCA conditions.

2.1 Modelling capability

2.1.1 Applicability

FRAPTRAN-1.3 allows the transient thermo-mechanical behaviour of boiling water reactor (BWR) and pressurized water reactor (PWR) fuel rods to be analysed. Material property data used are taken from the MATPRO material package, however, modifications exist, confer e.g. reference (FRAPTRAN-1.3, 2005). MATPRO comprises models for UO_2 as well as mixed $(U,Gd)O_2$ and $(U,Pu)O_2$ fuel, and both Zircaloy-2 and Zircaloy-4 materials. However, the fuel thermal conductivity correlation used in FRAPTRAN-1.3 includes neither the effect of Gd nor Pu on the conductivity.

Fuel rod LOCA analysis in FRAPTRAN applies a local model accounting for non-axisymmetric cladding deformations (ballooning) and an associated burst stress criterion. This high-temperature burst stress criterion, used in LOCA calculations, has been determined from experimental data on Zircaloy cladding material (Hagrman, 1981). Its validity for different treatments, such as cold-worked and recrystallization annealed conditions, is not clear. The material models in FRAPTRAN have not been designed or applied for detailed investigation of the differences in LOCA behaviour of Zircaloy and other Zr-based alloys.

For RIA calculations, an alternate criterion for low-temperature cladding failure is available. Pellet-cladding mechanical interaction (PCMI) in FRAPTRAN is modelled by perfect friction, i.e. in contact state, no relative sliding is permitted between fuel and cladding.

Two options are available for modelling of high-temperature cladding oxidation; (i) the Baker-Just and (ii) Cathcart-Pawel models. The Baker-Just oxidation model is intended for licensing calculations, whereas the Cathcart-Pawel model is aimed for best estimate calculations. Other models that are available as options in the FRAPTRAN code are (iii) a detailed model for calculating plenum temperature, (iv) a model for axial mixing of rod internal gases and (v) a facility to manipulate rod pressure by either providing a pre-defined fission gas release or a gas pressure history. The FRAPTRAN code has no fission gas release model.

The integral verification of FRAPTRAN-1.3 rests on data from 7 initially unirradiated fuel rods extracted from five different in-reactor LOCA experiments and 15 rodlets from Reactivity Initiated Accident (RIA) tests conducted in the French Cabri reactor and the Japanese Nuclear Safety Research Reactor (NSRR), see FRAPTRAN-1.3 (2005). The rodlets used for the RIA verification had fuel burnups ranging from 26 to 64 MWd/kgU. Previous version of the code has, in addition to LOCA and RIA tests, also been verified with data from 5 rods from four different irradiation experiments conducted in the Halden heavy-water boiling water reactor (HBWR) in Norway and 2 rods tested in the U.S. Power Burst Facility (PBF), Cunningham et al. (2001b).

2.1.2 Geometrical representation

In FRAPTRAN-1.3, the fuel rod geometry is represented by a column of cylindrical fuel pellets, which are located concentrically within a cylindrical cladding tube. The fuel pellets may be annular (equipped with central hole). The active length of the rod is divided into 1-25 axial segments, not necessarily of equal length. In case the rod geometry represents fresh fuel, the axial segments are assumed to have identical dimensions (diameters) and material properties. If the initial fuel rod geometry represents that of irradiated fuel, then the dimensions and material properties will vary for the axial segments. The thermal load, i.e. the heat generation varies from one axial segment to another. The clad tube is surrounded by a water/steam coolant, which has segment-wise uniform properties along the clad periphery, as shown in figure 2.1. In addition, a gas plenum volume is assumed at the top of the fuel rod.

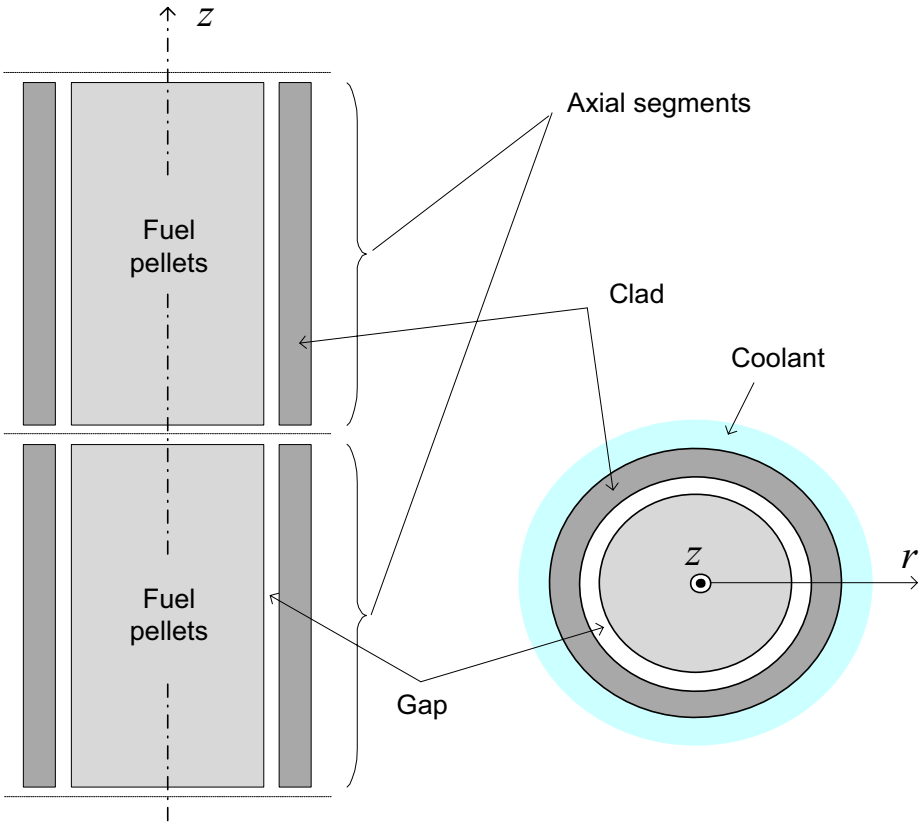

Figure 2.1: Geometrical representation of the fuel rod. Two axisymmetric axial segments of the rod are shown in the figure.

Fuel rod heat transfer and deformations are calculated for each axial segment individually, thus neglecting transfer of heat and mechanical forces between adjacent segments. This simplification, in combination with the assumed radial symmetry, makes the governing equations for heat transfer and deformations one-dimensional. Within each axial segment, the temperature and other variables are thus dependent on the radial coordinate only. The considered configuration is thus axisymmetric. However, in LOCA analyses a model accounting for local non-axisymmetric cladding deformation can be activated.

2.1.3 Time stepping

In FRAPTRAN-1.3, the transient heat transfer equation and the equations of mechanical equilibrium are solved for a sequence of time steps. A maximum of 20 time steps can be used to define the transient fuel rod power history. The axial and radial distributions of power are constant throughout the transient. General guidelines for selecting time step size for numerical solution of governing equations for various types of transient analyses are given in Cunningham et al. (2001a).

2.2 Thermal analysis

The thermal analysis in FRAPTRAN-1.3 involves calculation of the radial transient temperature distribution in each axial segment of the rod, as schematically illustrated in Figure 2.2.

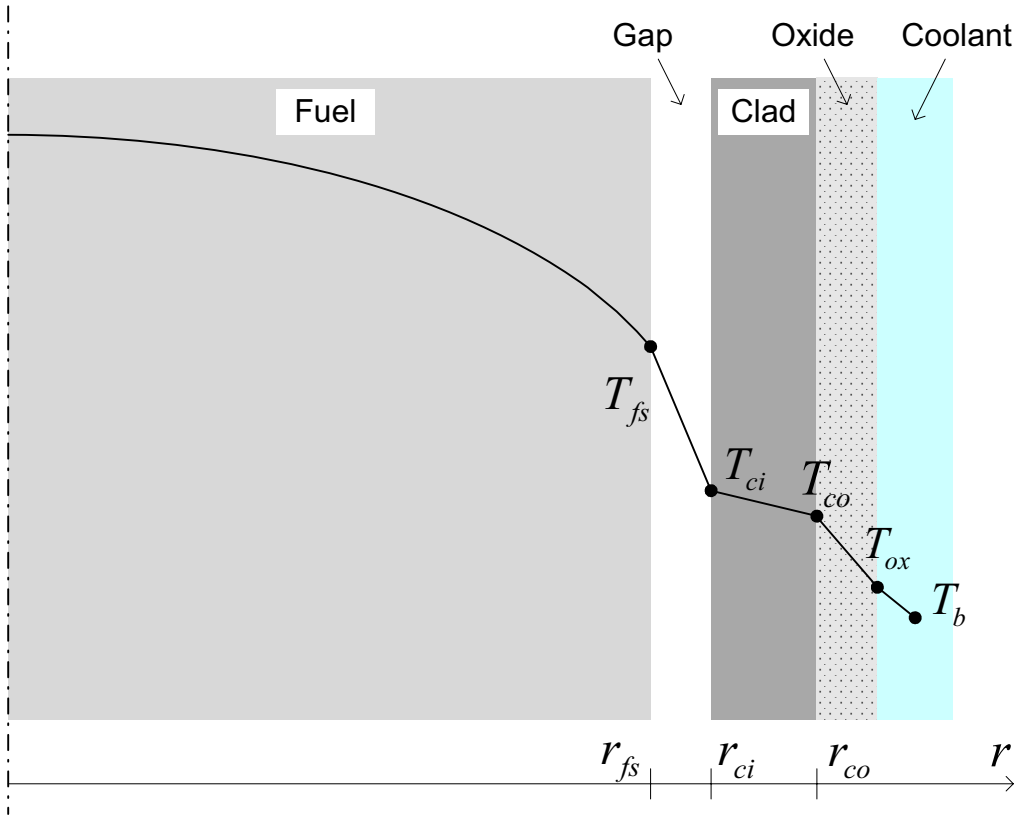

Figure 2.2: Schematic radial temperature profile in an axial segment of the rod.

Similar to FRAPCON-3, the heat transport within the rod is assumed to be purely radial. The heat flux within the fuel rod can thus be written

$$\vec{\phi} \;=\; \phi\, \vec{e}_r \,, \tag{2.1}$$

where ϕ is the radial heat flux and $\vec{e}_r$ the radial unit vector. The transient radial heat flux in the solids, i.e. in the fuel pellets, Zircaloy tube and oxide layer, is governed by the material properties; density ρ, heat capacity C_p and thermal conductivity λ for each material. The radial heat flux in the solids is related to the temperature through Fourier's law of heat conduction,

$$\phi \;=\; -\lambda \frac{\partial T}{\partial r}, \tag{2.2}$$

where T is the temperature and λ the thermal conductivity of the respective solid. At the pellet-to-cladding and oxide-to-coolant interfaces the radial heat flux is calculated from Newton's law of cooling. The time-dependent heat balance in FRAPTRAN-1.3 is described by the following equation

$$\rho \; C_p \frac{\partial T}{\partial t} \quad = \quad -\nabla \cdot \vec{\phi} \quad + \quad q \, . \tag{2.3}$$

The terms on right hand side of equation (2.3) represent the heat diffusion flux and the heat generation rate. The term on left hand side represents the instantaneous heat stored in the solid materials of the fuel rod, meaning that all heat generated in the rod is not immediately transported or released to the water coolant. This behaviour, i.e. the delay between the generated and released heats, is the sentence of the word *transient* (non-equilibrium). In *steady-state* (equilibrium), i.e. for $\partial T / \partial t = 0$, as for the fuel rod conditions modelled in FRAPCON-3, the stored energy is assumed to be zero, meaning that all heat generated in the rod is released to the coolant at each burnup/time step. Moreover, the radial distribution of the heat source q in FRAPTRAN-1.3 is assumed to be constant during a transient and is specified individually for each axial segment via code input. At the pellet-to-clad and oxide-to-coolant interfaces the radial heat flux is calculated from Newton's law of cooling

$$\phi \quad = \quad H \Delta T \, , \tag{2.4}$$

where H is a parameter called the surface conductance or the surface heat transfer coefficient and ΔT is the temperature difference across the interface. The local oxide-to-coolant (clad-to-coolant) heat transfer conditions for the rod can either be calculated by the coolant channel (fluid flow) model present in FRAPTRAN-1.3 or provided as prescribed data via code input. The modelling of the clad-to-coolant heat transfer is the topic of section 2.2.3.

2.2.1 Fuel pellet

The radial fuel pellet temperature distribution in FRAPTRAN-1.3 is determined in the same manner as in FRAPCON-3, that is, the heat conduction equation (2.3) is solved by using a finite difference method. The procedure of the temperature calculation is briefly described in the evaluation of the FRAPCON-3 code performed by Jernkvist & Massih (2002).

The fuel thermal conductivity model in FRAPTRAN-1.3 is based on the work of Ohira & Itagaki (1997). Ohira & Itagaki developed the conductivity correlation based on thermal diffusivity measurements on irradiated fuel and verified it against in-reactor fuel centreline temperature data. Later, Lanning et al. (2000) evaluated this correlation and introduced it in FRAPCON-3.2 with some modifications. This model is implemented also in the FRAPTRAN-1.3 program. The fuel thermal conductivity correlation in FRAPCON-3.2 is described by Jernkvist & Massih (2005).

Comment:
The effect of Gd and Pu on the fuel thermal conductivity is not included in the model used in FRAPTRAN-1.3.

2.2.2 Pellet-to-clad gap

The heat transfer across the pellet-to-clad gap is modelled in the same way as in FRAPCON-3 (Jernkvist & Massih, 2002).

2.2.3 Clad-to-coolant

The clad-to-coolant heat transfer is strongly dependent on the fuel rod wall temperature and coolant properties, such as mass flux, temperature and steam quality. For modeling the clad-to-coolant heat transfer, a number of heat transfer modes (regimes) with particular properties are formulated for each regime individually. This kind of clad-to-coolant heat transfer correlations are used in various thermo-hydraulics codes for reactor system analysis, such as RELAP5 (RELAP5, 2001), but also in fuel rod transient analysis codes like FRAPTRAN (Cunningham et al., 2001a), SCANAIR (Federici et al., 2000) and STAV-T (Jernkvist & Limbäck, 1995; Limbäck et al., 1998).

Supercritical heat transfer prevails if the clad wall temperature (T_w) exceeds the critical temperature T_c corresponding to the critical heat flux at cladding wall, j_c, which is the heat flux at departure from nucleate boiling (DNB). At DNB, the heat flux decreases rapidly with increasing wall temperature, until a stable vapour film is developed on the clad surface. The main heat transfer regimes are schematically illustrated in Figure 2.3.

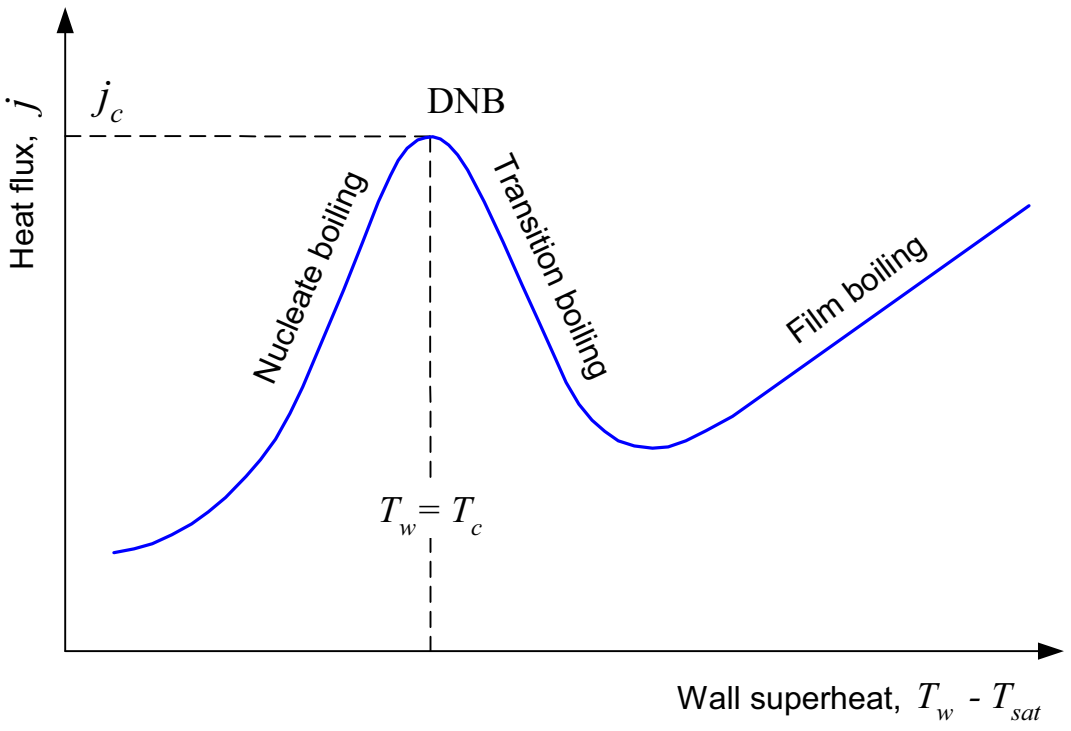

Figure 2.3: Sub- and supercritical heat transfer. The respective temperatures, T_w, T_c and T_{sat}, in the figure are the clad wall temperature, the temperature at the critical heat flux and the coolant saturation temperature, respectively.

In FRAPTRAN, the coolant conditions can either be specified as pre-calculated tabular data or be determined by a coolant channel model available in the code. More specifically, the clad-to-coolant boundary conditions for transient analysis are either defined by specifying a coolant condition option (`coolant='on'`) or a heat transfer coefficient option (`heat='on'`). The latter specification overrides the former, and all its associated suboptions, in case both options are given in the input file. Moreover, the clad-to-coolant instructions are defined in the boundary condition block (`$boundary`) of the input file and are described in appendix A and G of the FRAPTRAN manual (Cunningham et al., 2001a). However, the most important options for the specification of coolant boundary conditions, illustrated in the flowchart in figure 2.4, are outlined in the sequel.

The coolant conditions in the `coolant` option (defined above) can be calculated during the course of a transient rod analysis by the coolant channel model in FRAPTRAN or interpolated from existing data, produced by a thermo-hydraulics code such as RELAP5. The use of existing data for the clad-to-coolant boundary condition is selected by setting the input parameter `tape1` equal to an option number (>0). The cooling medium is assumed to be water. As an example, by specifying `tape1=1` in the input file, FRAPTRAN assumes a data file in which the following parameters are tabulated as a function of time; coolant pressure, coolant enthalpy and coolant mass flux. The exact format of the aforementioned data is given in Appendix G (section G.1) of the FRAPTRAN manual. The format of coolant data produced by a RELAP5 analysis can be directly used in FRAPTRAN by specifying `tape1=3`.

The coolant heat transfer coefficient in the `heat` option is invoked in the computations via tabulated data, which are given either directly in the input file or provided separately through a data file. The data file sub-option, assuming tabulated data on coolant pressure, coolant temperature and coolant heat transfer coefficient as a function of time, available on a file, is selected by setting the input parameter `tape2` to unity (`tape2=1`). Thus, the coolant medium in this case can be anything. The format of the tabular data is given in Appendix G (section G.2) of the FRAPTRAN documentation (Cunningham et al., 2001a).

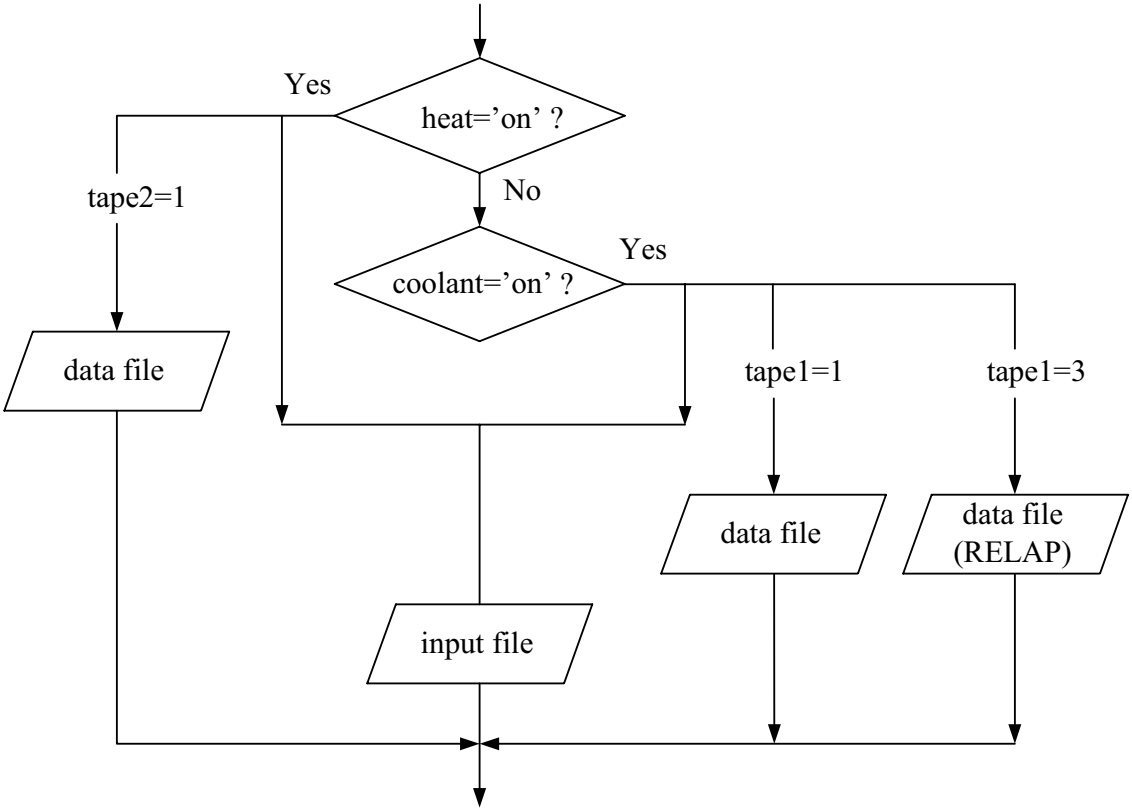

Figure 2.4: Main options for modelling of clad-to-coolant boundary conditions in FRAPTRAN-1.3. For more details, confer Cunningham et al. (2001b).

In case the coolant channel model of FRAPTRAN is utilized, the clad-to-coolant heat transfer coefficient during a transient is determined from a set of correlations depending on the heat transfer mode (figure 2.3). The correlations available in FRAPTRAN are listed in table 2.1 (Cunningham et al., 2001a). The default heat transfer correlation for film boiling mode is a combination of the Tong-Young and Condie-Bengtson correlations. The selection of a specific non-default correlation in the film boiling mode is described in appendix C. No options, i.e. alternate correlations, exist for the other heat transfer regimes listed table 2.1. The definition of the heat transfer regimes in this follows the terminology used in the FRAPTRAN documentation.

Heat transfer regime	Correlation
Forced convection to liquid	Dittus-Boelter
Nucleate boiling	Chen
High flow transition boiling	McDonough et al.
High flow film boiling	Groeneveld
	Doughall-Rohsenow
	Tong-Young
	Condie-Bengtson
Low flow boiling and free convection	Modified Hsu & Bromley-Pomeranz
Forced convection to superheated steam	Dittus-Boelter
Low-pressure film boiling	Doughall-Rohsenow

Table 2.1: Heat transfer correlations available in the coolant channel model of FRAPTRAN-1.3. For references, see Cunningham et al. (2001a).

The default critical heat flux correlation applied in FRAPTRAN-1.3 is a combination of the Westinghouse W-3, Hsu-Beckner and modified Zuber correlations. For saturated coolant conditions the critical heat flux is calculated by a combination of the W-3 and Hsu-Beckner correlations unless the coolant mass flux is below 270 kg/m^{2}s, then critical heat flux is computed by using the modified Zuber correlation. The set of critical heat flux correlation correlations available in FRAPTRAN-1.3 and their selection are defined in Appendix C.

Comment:
According to the developers of the FRAPTRAN-1.3 code the calculation of the coolant enthalpy using the coolant channel model is satisfactory for operational transients, but not for large and small break LOCAs and RIAs (Cunningham et al., 2001a). Their experience is that application of the coolant channel model causes difficulties in the numerical solution. However, we have not been able to assess their conclusion since currently we have no realistic LOCA case at hand and hence such an effort is beyond of scope in the present task. Moreover, Cunningham and co-workers recommend users of the code to use pre-calculated thermal-hydraulics data for the clad-to-coolant boundary condition, e.g. data calculated by the RELAP5 program (RELAP5, 2001).

2.2.3.1 Reflood heat transfer

The clad-to-coolant boundary conditions defined above prevail until a pre-defined (prescribed) instant (time) when reflood is to start. Once the reflood begins, all coolant boundary conditions are determined only by reflood option (Cunningham et al., 2001a).

2.3 Mechanical analysis

The main objective of the mechanical analyses in FRAPTRAN-1.3 is to calculate the fuel and clad deformations, which are necessary for accurate determination of the rod internal gas pressure, the pellet-clad contact pressure and the pellet-to-clad heat transfer. The clad deformation, in combination with its temperature, is a key parameter for accurate determination of the clad stress state. In LOCA analyses, the stress state is used to calculate the time to rupture and associated rupture stress (burst stress) of cladding tube.

Mechanical analyses in FRAPTRAN-1.3 are performed by use of rather simple models, taken from the FRACAS-I subcode, Bohn (1977). The models are based on small-strain theory, that is, analyses are thus restricted to small deformations. The fuel is treated as a perfectly rigid material, which swells or shrinks in stress-free condition due to thermal expansion. The fuel deformation is thus affected neither by restricting forces from the clad tube, nor by internal stresses in the fuel material.

2.3.1 Fuel pellet

The fuel pellet in FRAPTRAN is considered to be rigid (FRACAS-I subcode). This is the same model as is applied in FRAPCON-3 and has been outlined in an earlier report, Jernkvist & Massih (2002). Permanent deformations influencing the pellet diameter, such as athermal swelling due to accumulation of solid fission products, densification and fragment relocation calculated by FRAPCON-3, may be introduced via a special initialization file.

2.3.2 Clad tube

The cladding tube in FRAPTRAN is treated as a thin-walled structure with uniform temperature across the wall thickness. Depending on the stress state of the cladding, the deformations are either calculated by a global model or a combination of global/local cladding models (Cunningham et al., 2001a). The cladding in the global model is axisymmetric and considers the deformation of the entire tube, whereas the local model accounts for local non-axisymmetric deformations at a certain axial elevation (segment). The local modelling in FRAPTRAN is invoked when large cladding deformations and strains are predicted, e.g. to capture the non-axisymmetric deformation behaviour (ballooning) observed in LOCA tests. The clad ballooning model consists of thin-shell membrane elements.

The sum of clad permanent (plastic) deformation, i.e. time-independent plus time-dependent (creep) deformation in FRAPTRAN, is calculated by a Norton law stress-strain relationship (Hult, 1968). The plastic deformation calculated in the ballooning model accounts for cladding anisotropic properties by using the theory of Hill (1948), but not the axisymmetric cladding model. The thermal annealing effect of the clad mechanical properties is considered in the clad deformation models. The thermal annealing effect refers to the gradual reduction of cold work and effective neutron fluence (>1 MeV) at high cladding temperatures and is determined by using the MATPRO correlations (Allison et al., 1993).

A novelty in FRAPTRAN-1.3 relative to previous versions is that the effect of wall thinning, due to cladding oxidation, on cladding stresses has been included.

As in FRAPCON-3, the loading and deformation in the global model are assumed to be axisymmetric, and the shear components of stress and strain are neglected. The structural equations for calculation of displacements, stresses and strains follow the procedures of FRAPCON-3, see e.g. Jernkvist & Massih (2002). The deformation mechanisms considered in the clad tube are

- Elasticity
- Thermal expansion
- Time-independent plasticity and creep

We should recall that the stress (σ) and strain (ε) in the plastic region in FRAPTRAN is related by the power law

$$\sigma = K\varepsilon^n \left(\frac{\dot{\varepsilon}}{10^{-3}} \right)^m , \tag{2.5}$$

where K is the strength coefficient, n the strain hardening exponent, $\dot{\varepsilon}$ is the strain rate and m the strain rate sensitivity exponent.

The cladding mechanical properties applied in FRAPTRAN-1.3 are based on modified MATPRO models (Allison et al., 1993). These altered material models and other code changes relative to FRAPTRAN-1.2 have been documented in the FRAPTRAN-1.3 release document available for FRAPCON-3/FRAPTRAN users via internet at www.pnl.gov/frapcon3 (FRAPTRAN-1.3, 2005). Recent modifications to the FRAPTRAN code and their implications are also discussed in a paper by Geelhood et al. (2004). Appendix A provides an outline of the mechanical properties model in FRAPTRAN-1.3 and a comparison with the original MATPRO models.

The FRAPTRAN-1.3 cladding mechanical properties model discriminates between Zircaloy-2 and Zircaloy-4 materials and has been adapted for calculation of properties up to temperatures of 2100 K. The main difference of the modified model relative to that of previous version of FRAPTRAN pertains to the dependence of the strength coefficient (K) and strain hardening exponent (n) on neutron fluence. No limitation with respect to neutron fluence is given. Moreover, the strain rate sensitivity exponent has been simplified relative to that proposed in MATPRO (Allison et al., 1993).

The effects of oxygen on cladding plastic deformation are included by correlations for the changes in the correlations for the strength coefficient, strain hardening exponent and the strain rate sensitivity exponent with increasing oxygen content. The correlations, modelling the influence of cladding oxygen content, enhance the values of these three material property parameters (Allison et al., 1993). The base correlations for K, n and m, used in FRAPTRAN-1.3, are outlined in appendix A.

Comment:
The mechanical properties model is restricted to Zircaloy-4 and Zircaloy-2 material. Hence, it lacks support for other zirconium-based alloys.

Elasticity and thermal expansion:
Young's modulus, Poisson's ratio and the coefficients of thermal expansion for the cladding material are calculated by using correlations from the MATPRO package (Allison et al., 1993).

Time-independent plasticity:
The method for calculation of cladding plastic strain increments is in FRAPTRAN-1.3 performed in the same manner as in FRAPCON-3 (Jernkvist & Massih, 2002). The cladding mechanical model has been validated against yield stress and ultimate tensile strength values obtained from uniaxial and biaxial material tests, i.e. for the PNNL database of mechanical properties. The database comprises axial and ring tensile tests as well as burst tests. Figure 2.5 shows a comparison of calculated yield stress with ring tensile test data on irradiated stress-relieved Zircaloy-4 at two different strain rates, 0.01 and 5 s^{-1} and in the temperature range from 20 to 600°C (Desquines et al., 2005). The cladding samples in the actual tests were extracted from high-burnup 17×17 fuel assembles with average burnups ranging from 54 to 64 MWd/kgU. In the FRAPTRAN-1.3 model, a fluence of 8×10^{25} m^{-2} and cold work of 50% was assumed.

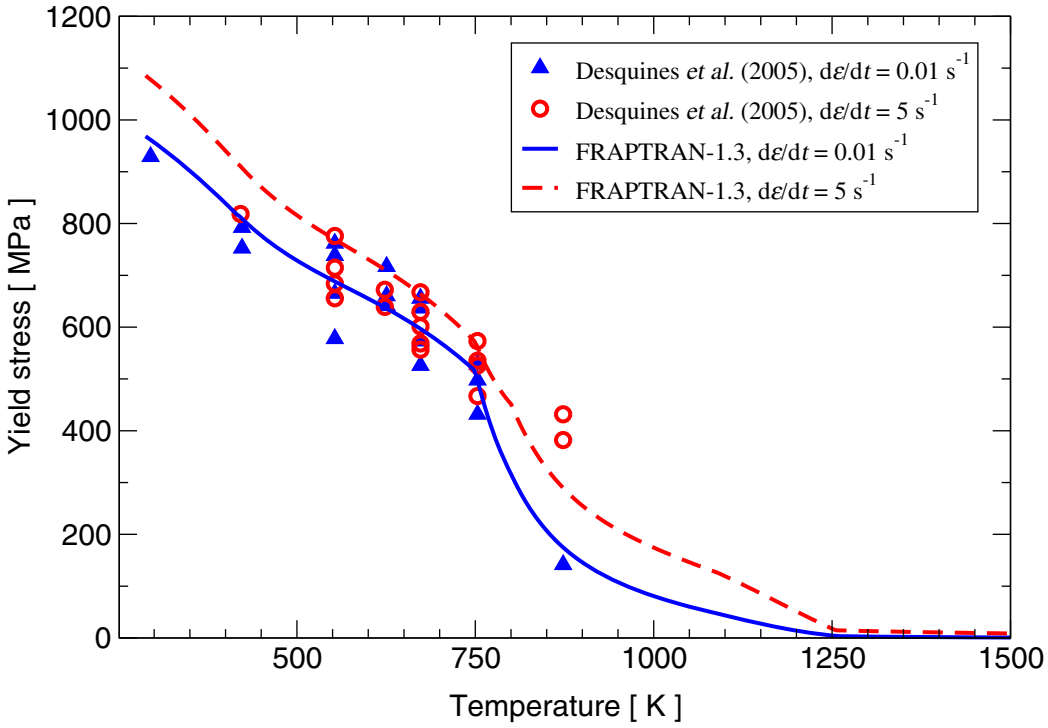

Figure 2.5: Comparison of calculated yield stress with data from irradiated Zircaloy-4 samples tested in the PROMETRA program (Desquines et al., 2005). A fast fluence of 8×10^{25} m^{-2} and a cold work of 50% are applied in the FRAPTRAN-1.3 model.

Comment:
Since the basis (PNNL database) for the models is not described in the available FRAPTRAN documentation we have not been able to assess the ranges of validity of the material properties model.

For each test in the database, besides cladding material, the following test conditions would be needed for proper assessment of the model, (i) type of test, (ii) test temperature, (iii) load and (iv) neutron fluence. The model lacks validation for Zr-Nb alloys. For LOCA application, material property data up to at least 1500 K has to be covered, i.e. to considerably higher clad temperatures than in the PROMETRA tests (figure 2.5) and also higher than in the assessment presented by Geelhood et al. (2004).

Creep:
The strain rate sensitivity of the cladding mechanical model in FRAPTRAN-1.3 has been assessed by comparing calculated yield stress as a function of temperature with yield stress data obtained at different strain rates and temperatures in the PROMETRA program (Geelhood et al., 2004; FRAPTRAN-1.3, 2005). More specifically, the capability to calculate yield stress over a temperature range from 293 to 1373 K, strain rates from 0.01 to 5 s^{-1} and neutron fluences from 6×10^{25} to 8×10^{26} m^{-2} has been demonstrated.

Comment:
Recently published data from the PROMETRA program cover mechanical property tests in addition to irradiated Zircaloy-4 also for the M5 and standard ZIRLO cladding materials (Cazalis et al., 2005). Although, the maximum cladding temperature in the PROMETRA tests is not so high, the tests should be considered in a tentative application of the FRAPTRAN code, also for Zr-Nb alloys.

In order to distinguish the high-temperature creep behaviour between current cladding materials, the differences in the kinetics of $\alpha\rightarrow\beta$ and $\beta\rightarrow\alpha$ phase transformations of zirconium alloys has to be considered. This is an important issue in LOCA assessment of fuel rods, since the niobium addition in zirconium-base alloys lowers the $\alpha\rightarrow\beta$ transition temperature relative to Zircaloy cladding materials. The earlier transition to β phase may enhance the amount of thermal creep deformation under LOCA in fuel rods equipped with Nb-alloyed cladding materials compared to rods with Zircaloy claddings. Moreover, the impact of hydrogen and oxygen on phase transformations should also be considered in a high-temperature cladding material model for LOCA assessment (Massih, 2007).

2.4 Clad oxidation

FRAPTRAN-1.3 contains two alternate models for calculation of cladding oxidation behaviour at high temperatures, namely the (i) Baker-Just and (ii) Cathcart-Pawel models. If the metal-water reaction option in FRAPTRAN-1.3 is turned on (`metal='on'`) and one of the aforementioned oxidation models is chosen, the following data pertaining to clad high-temperature oxidation are written for each axial segment in the output file:

- Outer diameter (OD) oxide thickness,
- Inner diameter (ID) oxide thickness,
- OD oxygen uptake,
- ID oxygen uptake,
- Total equivalent cladding reacted and
- Metal-water reaction energy.

The measure of the amount of cladding wall thickness consumed or reacted in the oxidation process is termed *equivalent cladding reacted* (ECR) and includes the oxidation of both inner and outer tube surfaces. The Baker-Just oxidation model is intended for licensing calculations, whereas the Cathcart-Pawel model is aimed for best estimate calculations. The Baker-Just and Cathcart-Pawel models, their bases and associated design criteria for assessment of fuel rod behaviour under LOCA are discussed in a separate report, Massih (2007). Moreover, the energy generated by the exothermic zirconium water reaction is calculated for each axial segment and applied as heat source in the thermal calculations.

2.4.1 Baker-Just

The total ECR calculated by FRAPTRAN-1.3 includes, in addition to the oxidation at the cladding inner and outer surfaces calculated during a transient event, the existing initial oxide thicknesses of the cladding, i.e. prior to transient. The initial oxide layer thicknesses at the cladding inner and outer diameters are prescribed in the input file for a FRAPTRAN-1.3 analysis. More specifically, the progress of the oxide layer thickness (w) by the Baker-Just model during a time step (Δt) is calculated in FRAPTRAN-1.3 by

$$w^{t+\Delta t} = w^{t} + \sqrt{A \exp(-Q/RT)\Delta t}\,, \tag{2.6}$$

where w^t is the oxide layer thickness at time t, A is a constant in units of m^2/s, Q the activation energy, R the gas constant, T the cladding temperature and t the time. The values of the parameters used in the Baker-Just correlation in FRAPTRAN-1.3 are given in table 2.2 below.

Parameter	Symbol	Value
Oxidation constant	A	1.885×10^{-4} m^2/s
Activation energy	Q	45500 cal/mol
Gas constant	R	1.987 cal/mol/K

Table 2.2: Parameters used in the Baker-Just model in FRAPTRAN-1.3.

The accumulated mass of oxygen m in the unit of kg/m^2 at the cladding surfaces at advanced time ($t+\Delta t$) is calculated by

$$m^{t+\Delta t} = (w_{OD}^{t+\Delta t} + w_{ID}^{t+\Delta t})\rho_{ZrO_2} f_1\,, \tag{2.7}$$

where ρ_{ZrO2} is the density of ZrO_2 and f_1 the atomic weight fraction of oxygen in zirconium oxide (ZrO_2). The respective values for ρ_{ZrO2} and f_1 applied in the code are 5680 kg/m^3 and 0.26.

The total ECR fraction (f_{ECR}), at each axial rod segment in FRAPTRAN-1.3, is calculated from the ratio of the cladding oxygen masses in the oxide and the metal, i.e. by

$$f_{ECR} = \frac{m^{t+\Delta t}}{(R_{OB} - R_{IB})\rho_{Zr} f_2}, \tag{2.8}$$

where R_{OB} and R_{IB} are the respective radial loci of the cladding outer and inner oxide/metal boundaries, ρ_{Zr} = 6560 kg/m^3 the density of zirconium and f_2 = 0.35 the weight fraction of oxygen in zirconium.

2.4.2 Cathcart-Pawel

The Cathcart-Pawel equations for high-temperature oxidation comprise basically three different correlations, one for calculation of the oxide mass gain at clad surface, one for the oxide layer thickness and one for the thickness of the oxygen-stabilized α-phase zirconium below the outer clad oxide layer. The calculation of ECR follows the same procedure as has been described for the Baker-Just model. For a review of the Cathcart-Pawel model, see Massih (2007). Moreover, the Cathcart model applied in FRAPTRAN-1.3 follows the method documented in MATPRO (Allison et al., 1993).

For verification of the calculation of oxide layer build-up by the Cathcart-Pawel model implemented in FRAPTRAN-1.3, we utilized data from a series of steam oxidation tests, reported by Erbacher & Leistikow (1987). In these tests, unirradiated Zircaloy-4 tube specimens were subjected to three different double-peaked transient temperature variations, see figure 2.6, and the oxide mass gain at three different instants in time during each test was measured. The temperature levels during the second peak in the respective tests, 1, 2 and 3, were 1000, 1100 and 1200°C (figure 2.6). The outer diameter and the wall thickness of the tube specimens were 10.75 and 0.725 mm, respectively. Moreover, the as-fabricated oxygen concentration in the tube material was assumed to be 1200 ppm in the computations.

The calculated oxide mass gain as a function of time for the tests is compared with experimental data in figure 2.7. We note that the measured oxide mass gain after the first peak (0.44-0.49 mg/cm^2) is slightly underestimated by the model, whereas the measurements at begin and end of the hold period of the second peak are overestimated. The overestimation by the model at the end of the tests varies between 16 and 27%.

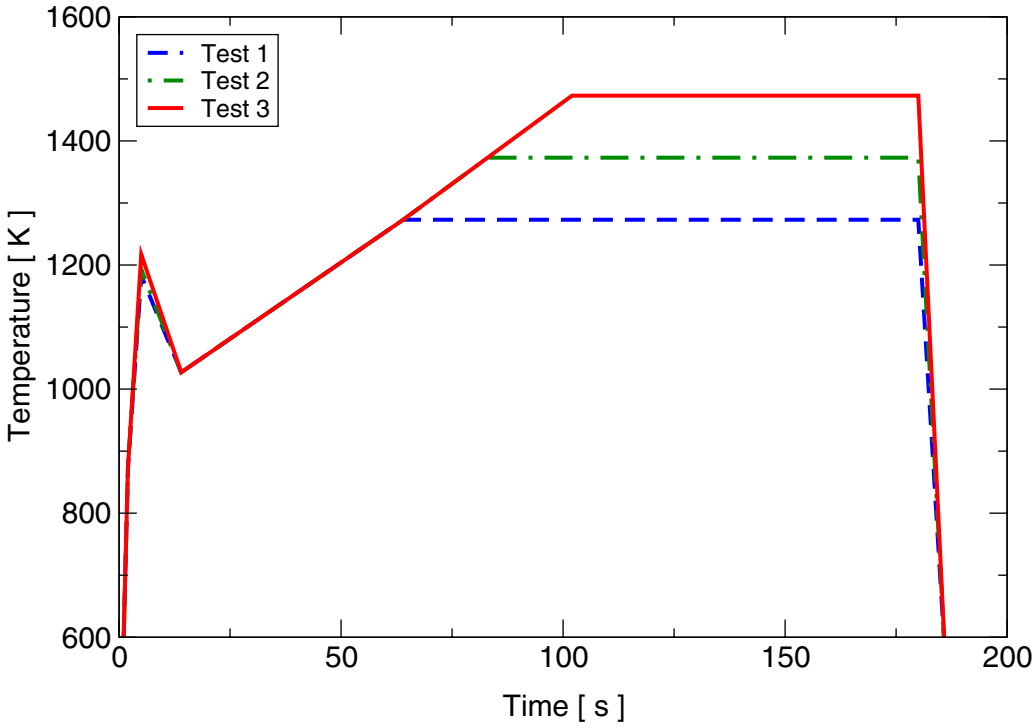

Figure 2.6: Transient temperature histories used in the steam oxidation test on Zircaloy-4 tubing employed by Erbacher & Leistikow (1987).

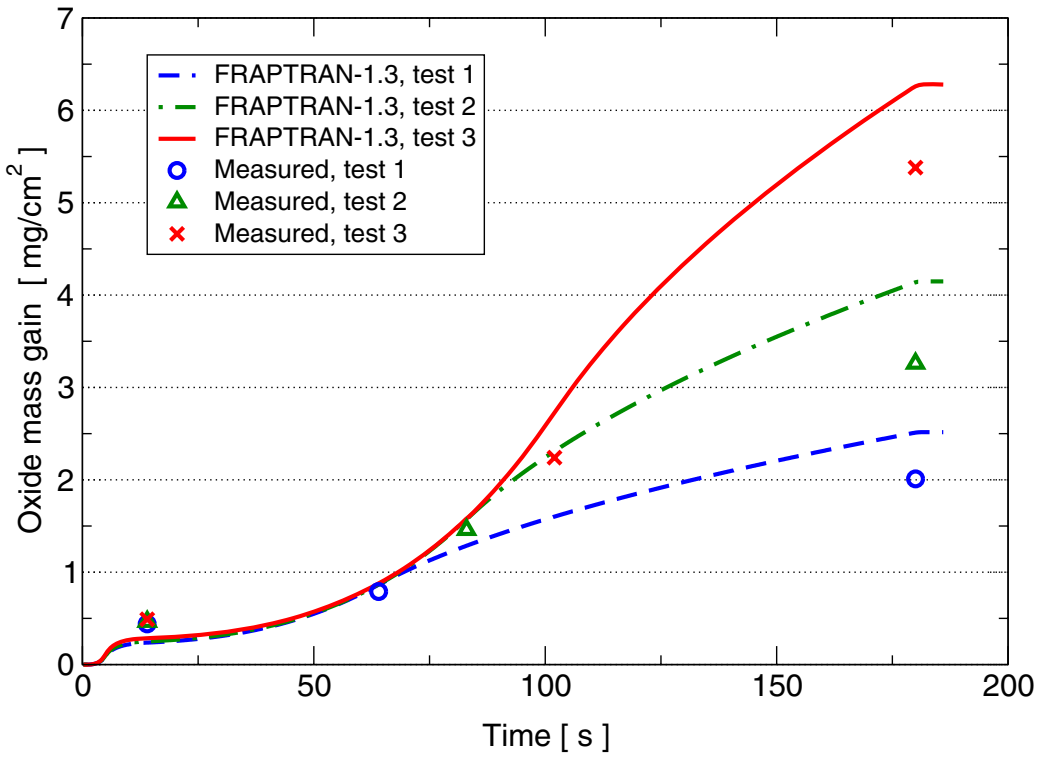

Figure 2.7: Calculated oxide mass gain for Erbacher & Leistikow's tests (1987) by using the Cathcart-Pawel model in FRAPTRAN-1.3.

Comment:
The oxidation kinetics of the Cathcart-Pawel model should be evaluated for cladding temperatures higher than the maximum temperature of 1200°C used in the Erbacher & Leistikow's (1987) tests. A good starting point for this purpose would be the oxidation tests published by Pawel et al. (1980) with peak clad temperatures between 1000 and 1400°C. More specifically, the tests reported by Pawel and co-workers involve Zircaloy-4 tube specimens subject to different kinds of single and double-peaked temperature excursions.

The effect of oxygen in the Zr matrix on the α-to-β phase transformation and associated kinetics should be included in the high-temperature oxidation calculation in FRAPTRAN. This is a prerequisite to be able to capture differences in the high-temperature LOCA behaviour of Zircaloys and other zirconium-base cladding materials, such as Zr-Nb alloys. Relevant models for this purpose can be found in Massih (2007). The Cathcart-Pawel model in FRAPTRAN-1.3 includes a simplified calculation of the oxygen concentration across wall thickness, however, its predictive capability and interaction with other models is unknown. This particular model should also be further investigated.

2.5 Failure models

FRAPTRAN-1.3 employs different models for prediction of clad failure depending on the cladding temperature and amount of cladding plastic hoop strain. The failure models are intended only for Zircaloy cladding material.

2.5.1 PCMI-driven failure

For transients where the cladding deformation is primarily driven by the pellet-cladding mechanical contact pressure, a failure model based on uniform plastic hoop strain is used. This strain-based failure model, described in detail by Geelhood et al. (2004), is a function of cladding temperature and excess hydrogen concentration, i.e. hydrogen concentration above the solubility limit. In the same paper, the capability of the model to retrodict failure of various pulse reactor tests simulating reactivity initiated accidents (RIA) is also elucidated. Additional clarification regarding the applicability and validity of the model is given in the FRAPTRAN-1.3 release document (FRAPTRAN-1.3, 2005).

2.5.2 Balloning type of failure

Clad failure as a consequence of large hoop plastic strains, i.e. due to ballooning type of deformation such as anticipated under a postulated LOCA is calculated by the BALON2 model (Hagrman, 1981) in FRAPTRAN-1.3, figure 2.8. The BALON2 model determines the non-axisymmetric cladding shape and potential rupture from wall thinning. If the cladding has a hot spot due to circumferential temperature variation, the deformation will be localized at the hot spot. The theoretical basis and verification of the ballooning model is described in Hagrman (1981). Similar models for calculation of clad deformations under LOCA have been published by Rosinger (1984) and Uchida (1984).

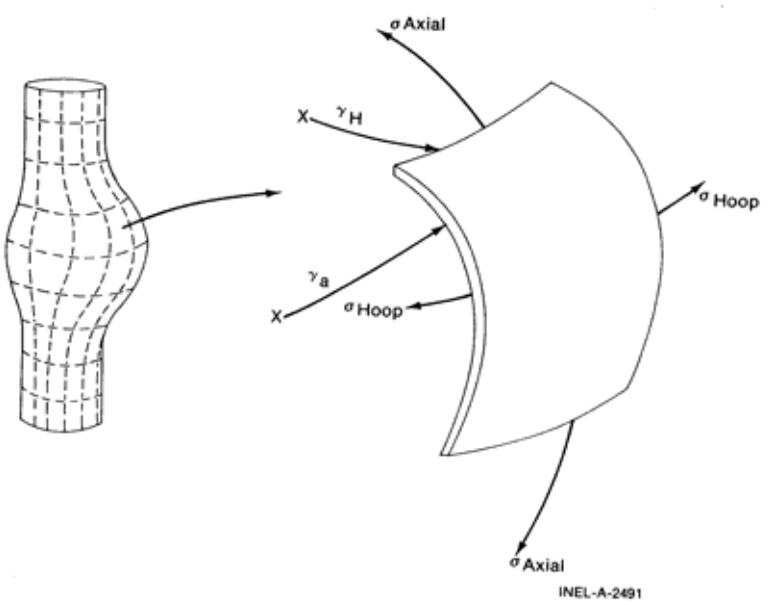

Figure 2.8: Illustration of the ballooning model in FRAPTRAN. After Cunningham et al. (2001a).

The clad deformation under LOCA is driven by high rod gas overpressure and increasing cladding temperature until efficient fuel rod cooling conditions are established. The FRAPTRAN model assumes that, if a clad instability strain is exceeded in any axial segment of the rod, then the cladding cannot maintain its cylindrical shape and local ballooning occurs. For the axial segment at which clad instability is predicted, a large deformation ballooning analysis is initiated. The calculation of local cladding deformations is switched on when the effective plastic strain, calculated in the global model, exceeds a uniform clad instability strain given by MATPRO (Allison et al., 1993). Furthermore, the ballooning model allows for non-axisymmetric large deformation of the cladding and can take into account local axial and circumferential temperature variations. Local heat transfer coefficients are calculated as the cladding ballooning progresses and additional surface area is presented to the coolant. High temperature cladding rupture in BALON2 is predicted by a burst criterion, in which clad failure is assumed as soon as the calculated local hoop stress reaches a critical burst stress, also given by MATPRO (Allison et al., 1993). This type of combined global/local model approach to quantify local phenomena in fuel rods is computationally efficient and has also been applied for LOCA assessment by Jernkvist & Limbäck (1995) within a two-dimensional finite element framework.

The burst stress criterion in BALON2 is a function of temperature and the strength coefficient for fully annealed Zircaloy cladding (Hagrman, 1981; Allison et al., 1993). We note that the formulation of the strength coefficient in Hagrman (1981) contains only the temperature and cold work dependencies of the strength coefficient used in the FRAPTRAN-1.3 code and a single linear dependency on effective fast neutron fluence (>1 MeV) valid for all fluence levels, see Appendix A.

The burst stress criterion is not affected by heating rate or strain rate, but to some extent by irradiation and cold work. More specifically, for cold worked or irradiated cladding, the burst stress is increased by four tenths of the increase of the strength coefficient due to irradiation and cold work.

Comment:
The verification of the BALON2 model rests on a number of separate effects LOCA tests initially documented by Hagrman (1981) and also summarized in MATPRO (Allison et al., 1993). The database used for the development of the BALON2 model comprises data mainly from pressurized transiently heated unirradiated cladding specimens, but also from two in-reactor tests; one performed in the German FR2 reactor and one in the U.S. Power Burst Facility (irradiation effects test PBF IE-5). The burst stresses in the tests ranged from 477 to 1487 K. To the best of our knowledge, the BALON2 model has not been subject to any renewed assessment against separate effects tests since then, despite certain material models affecting the ballooning behaviour have been modified. Hence, it would be sound to reassess the capacity of the model in light of its current basis and also other published data, see e.g. the works by Jernkvist & Limbäck (1995) and Limbäck et al. (1998).

The burst strain as a function of burst temperature from LOCA experiments at a given heating rate exhibits a characteristic double-peaked behaviour with a minimum in the (α+β)-phase region, see e.g. the tests reported by Rosinger (1984) on Zircaloy cladding. The capability to calculate this type of behaviour is essential for LOCA analysis, but has not been reported for the BALON2 model in FRAPTRAN. Thus, the effect of burst strain versus burst temperature response of BALON2 should be calculated, for different levels of heat rate, and compared to experimental data, e.g. the data reported by Rosinger (1984) and more recent data reviewed in Massih (2007) could be used. Moreover, Hagrman's verification of the BALON2 model contains a very limited verification of the effect of burst strain on circumferential temperature variation. His verification comprises transiently heated Zircaloy cladding specimens up to a heating rate of 30 Ks^{-1}. This verification should be extended to heating rates up to at least 100 Ks^{-1}, and should also cover at a least the burst behaviour in the (α+β) and β phase regions (Rosinger, 1984; Ferner & Rosinger, 1985). In order to compare the burst behaviour of different cladding materials, the high-temperature cladding deformation model in FRAPTRAN, must account for different creep rates in the α, (α+β) and β phase regions of the material. A prerequisite for distinguishing creep rates in the α, (α+β) and β phase regions is a model calculating the fraction of cladding wall in the respective phase regions under transient conditions.

In the BALON2 model description (Hagrman, 1981) it is recommended that we should not apply the additional correlations in the MATPRO package that account for clad oxidation in the mechanical properties of cladding. The model does not treat multi-layered cladding (oxide layers, oxygen-stabilized α layers and β layer). However, the effect of oxygen in the material properties should be included in the burst model, since it plays an important role in the cladding burst behaviour. A model for burst prediction under LOCA, including the oxygen effect, has been published for instance by Rosinger (1984).

Finally, the BALON2 model itself lacks verification of the time to cladding rupture and associated rupture strain from separate effects LOCA experiments on internally pressurized and transiently heated cladding specimens. This kind of tests can be successfully used to qualify material models for integrated fuel rod LOCA prediction (Jernkvist & Limbäck, 1995; Limbäck et al., 1998).

3 FRAPTRAN-1.3 interface

3.1 Input

The input data needed by FRAPTRAN-1.3 are entered via an *input file* and optionally also a separate *data file* containing clad-to-coolant boundary conditions. Both these files are in text format. Thus, the clad-to-coolant boundary conditions for FRAPTRAN-1.3 can either be specified in the input file or by means of a data file. In cases, where the clad-to-coolant heat transfer conditions are determined by an external thermo-hydraulics code it is convenient to import the data via the data file option. Keywords are used for entering various parameters in the input file, and by setting a switch to the desired system of units, parameter values can be given in either SI- or British units. The input file contains basically the following data

- Fuel rod dimensions and design information
- Transient power history, radial and axial power shapes
- Clad-to-coolant boundary conditions
- Discretization and modelling options

Furthermore, fuel rod initial conditions at a certain burnup for transient analysis with FRAPTRAN-1.3 may be streamlined from the output of a FRAPCON-3 calculation (Cunningham et al., 2001a).

The case definition in the input file is divided by eight blocks described in table 3.1. A data block is embraced by the block name and an end marker, `$end`, both given on new lines. Note that each of these data blocks must be defined in the input file even if they are empty.

Block name	Description
`$begin`	Case control parameters
`$iodata`	Input and output control parameters
`$solution`	Solution control parameters
`$design`	Fuel rod design data
`$power`	Power generation data
`$model`	Model selection parameters and data
`$boundary`	Coolant and clad-to-coolant boundary condition parameters and data
`$tuning`	Tuning parameters

Table 3.1: Data blocks defining a case in FRAPTRAN-1.3 input file.

The third input block contains data on the model size and radial/axial discretization to be used in the analysis. In FRAPTRAN-1.3, there are several limitations on the allowable problem size, as shown in table 3.2.

Parameter	Allowable range
Time steps (transient power history)	1-20
Axial segments	1-25
Axial power profiles	1
Radial power profiles	1
Radial fuel nodes in thermal analysis	2-30
Radial cladding nodes in thermal analysis	2-20

Table 3.2: Limitations on model size parameters in FRAPTRAN-1.3.

3.2 Output

Output from FRAPTRAN-1.3 is provided in the form of tabulated data.

3.2.1 Tabulated data

FRAPTRAN-1.3 provides tabulated output data on the calculated fuel rod thermal-, mechanical and gas response in the following forms

- Coolant condition data
- Integral fuel rod data
- Axial segment data
- Radial nodal temperature distributions per axial segment

All tabulated data are written on a single text file, time step by time step. Similar to the input procedures, there is a switch for obtaining output either in SI- or British units.

Coolant condition data per axial segment comprise enthalpy, pressure, mass flux, temperature, specific volume and steam quality. The integral rod data consist of e.g. average rod power, cladding axial extension, total free gas volume. The axial segment data present local information on power and calculated variables, such as radially averaged fuel enthalpies, cladding average temperatures, cladding stresses and strains, internal gas pressure, gas gap widths and conductances, high-temperature oxidation parameters, coolant properties and many more.

Rod radial temperature distributions are also presented segment-wise. Note that rod gas pressure is given per axial segment, since this parameter may vary axially if the axial gas mixing model is activated. Moreover, the plenum gas pressure is output as a separate parameter.

Comment:
The availability of detailed output from clad ballooning calculation is not clear.

3.2.2 Graphical output

The most important fuel rod parameters can be plotted graphically by using the Microsoft Excel plot program provided along with the FRAPTRAN code to users, via the internet at www.pnl.gov/frapcon3.

3.3 Interface to FRAPCON-3

FRAPTRAN-1.3 has the capability to import burnup-dependent initial condition data calculated by FRAPCON-3. This option is controlled by options in the case control (`$begin`) and input/output (`$iodata`) data blocks of input file. For details, see Cunningham et al. (2001a).

3.4 Interface to RELAP

FRAPTRAN-1.3 has the capability to import clad-to-coolant boundary conditions data produced by the thermal hydraulics code RELAP (RELAP5, 2001). The modelling options to include the boundary condition data file created by RELAP into a transient fuel rod analysis with FRAPTRAN are outlined in section 2.2.3.

4 Code implementation and documentation

4.1 History

The FRAPTRAN code was developed for the U.S. Nuclear Regulatory Commission (NRC) by the Idaho National Engineering and Environmental Laboratory (INEEL) and Pacific Northwest National Laboratory (PNNL). The FRAPTRAN code is the successor to the FRAP-T code series developed in the 1970s and 1980s. The last version in the FRAP-T series, FRAP-T6, was completed in the early 1980s (Siefken et al., 1981). The material properties package MATPRO, which is applied in the FRAP-T and FRAPTRAN codes, also date back to the 1970s.

In 1997, PNNL began the development of the FRAPTRAN code starting from FRAP-T6, version 21. Major changes incorporated in FRAPTRAN relative to FRAP-T6 include burnup-dependent material properties and models, simplification of the code and correction of errors identified since FRAP-T6 was released (Cunningham et al., 2001a-b). The current version of FRAPTRAN, version 1.3, was released in August 2005 (FRAPTRAN-1.3, 2005).

4.2 Code structure

The computational flow in FRAPTRAN-1.3 is shown in figure 4.1. The calculation starts by processing input data. Next, the initial fuel rod state for transient analysis is determined through a steady-state initialization calculation. Time is advanced according to the input-specified time step data, a transient solution is performed and a new fuel rod state is established. The new fuel rod state provides the transient initial conditions for the next time step. The calculations are repeated in this manner for time steps defined by the input-specified transient power history until a specified problem end time is attained. The default solution, i.e. using the default set of model parameters, for each time step consists of

1) Calculating heat conductance across pellet-clad gap and temperatures of fuel, clad and coolant
2) Calculating fuel and clad deformations
3) Calculating fuel rod void volume and internal gas pressure
4) Calculating local clad ballooning (if clad instability strain has been exceeded)

Additional calculations that can be activated, via model input options, in the transient solution comprise

- Calculating plenum temperature due to energy exchange between plenum gas and structural components
- Calculating axial transient flow of gases within the rod
- Calculating high-temperature oxidation
- Modifying rod gas pressure according to input-specified fission gas release (FGR) or gas pressure time history

Each of these calculations is made via separate high-level subroutines, represented by boxes in figure 4.1. The default and optional calculations executed during a transient solution are indicated by shaded and unshaded boxes, respectively. The fuel rod response for each time step is determined by repeated cycling through separate inner loops for the thermal and mechanical calculations within an outer loop for the combined (thermo-mechanical) solution, until convergence is achieved. The calculations of fuel rod temperature, deformation and gas pressure, and optionally axial gas mixing, shown in figure 4.1, are performed individually by loops over the number of axial segments.

The temperature distribution feeds the deformation calculation influencing the fuel and cladding thermal expansions and the cladding stress-strain relation. Permanent cladding strains (plastic plus creep) are obtained in the deformation calculation. If activated, the axial gas flow calculation is influenced by the calculated gas gap temperatures and widths. The pellet-clad gap conductance is determined in conjunction with the fuel rod temperature calculation.

The plenum thermal model calculates the plenum temperature considering the energy exchange between the plenum gas and structural components. The structural components considered consist of plenum spring, end pellet and cladding. Moreover, the energy exchange is assumed to occur by natural convection, conduction and radiation. If the plenum temperature calculation is bypassed, a plenum gas temperature of 10 K higher than the local coolant temperature is assumed. Moreover, the equations of the detailed calculation of plenum temperature are outlined in Cunningham et al. (2001a).

The high-temperature oxidation of cladding is either calculated by the Baker-Just or Cathcart-Pawel model, see section 2.4. Note that FRAPTRAN has no model to calculate transient release of fission gases. However, by specifying the fission gas release or gas pressure as a function of time, in the model data block of the input file, the rod pressure (and gas composition) can be manipulated during a transient simulation.

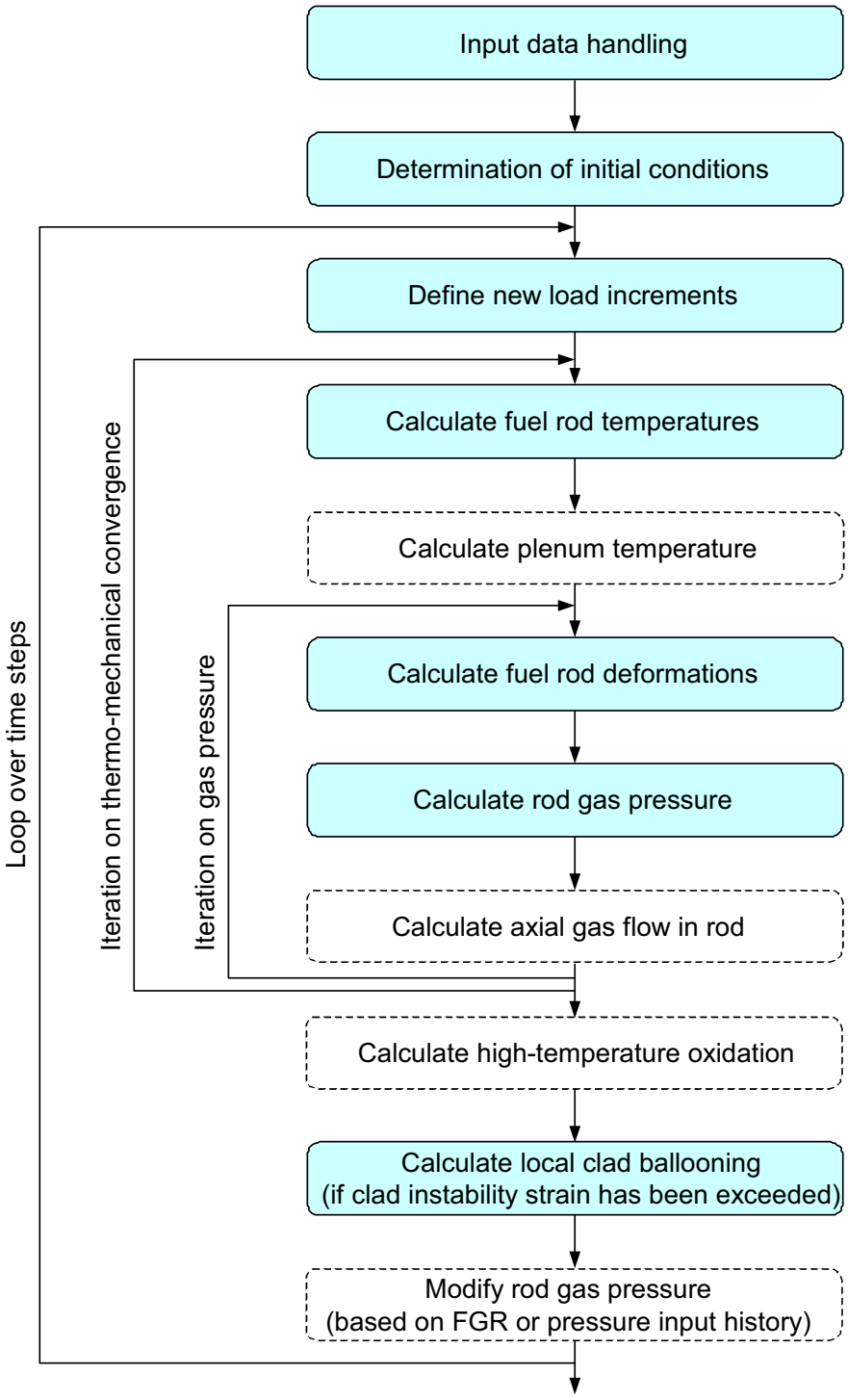

Figure 4.1: Flowchart of FRAPTRAN-1.3. The shaded boxes are calculations (tasks) executed by default and unshaded boxes tasks activated via code input.

4.3 Programming language and style

Similar to FRAPCON-3, the FRAPTRAN-1.3 code has over the past three decades been developed in various computer environments by using different versions of the Fortran programming language. Although the FRAPTRAN code has a modularized structure, starting from the main routine (*fraptran.f*), it is far from obvious where the different high-level loops in the program begin. This difficulty is primarily attributed to the wide use of "`if`" and "`goto`" statements in the source code and secondarily to the absence of proper comments indicating start and end of the loops. The scarcity of indication of loop ends in the program also makes it difficult to identify and distinguish the various convergence criteria applied in the code.

Since the code has had multiple developers during the years, its source naturally has different programming styles. The subroutines contain a mixture of SI, British and some unusual units giving rise to many unit conversions. In most cases, the conversion factors between units are logically defined by data command definitions, however, many cases still exist where unit conversions are hard-coded locally, without any comments, in mathematical expressions throughout the code.

4.4 Code documentation

There are two documents describing FRAPTRAN and its application

- A general code description, which briefly presents models, computational methods and code structure, Cunningham et al. (2001a)
- An integral assessment report, which presents the performed verification of the code, Cunningham et al. (2001b)

The current release of FRAPTRAN, version 1.3, is documented in a short note available at www.pnl.gov/frapcon3 (FRAPTRAN-1.3, 2005). Thus, the two aforementioned FRAPTRAN documents pertain to an earlier version of the code. Similar to FRAPCON-3, the MATPRO material properties package is used extensively also in FRAPTRAN. For our evaluation of FRAPTRAN-1.3 we have used the MATPRO version available at www.pnl.gov/frapcon3 (Allison et al., 1993).

The above documents give a good overview of the code, its modelling bases and validation. However, as for FRAPCON-3 (Jernkvist & Massih, 2002), many details in the documents do not correspond to the actual content of the source code; over the years, the code has been modified without introducing adequate changes in the documents. Moreover, certain information is scarce in the aforementioned documents. Similarly, as concluded in the previous evaluation of the FRAPCON-3 code performed by Jernkvist & Massih (2002) additional and updated documentation is also desirable for the FRAPTRAN code. Firstly, a user's manual to FRAPTRAN-1.3 would be helpful, in which guidelines on installing and running the program are given together with a thorough description of input and output. Here, simple sample cases of the major modelling options to show the code's capability could be demonstrated, e.g. clad-to-coolant condition, gas mixing, interface to FRAPCON-3 initialization file, etc.

Secondly, a maintenance manual or programmer's manual is desirable for those who intend to modify or extend the code. There is a significant gap between the general code description and the Fortran source code, which could be bridged by such a manual.

5 Supporting database

The spectrum of verification cases used for recent versions of the FRAPTRAN code is summarized in table 5.1. The LOCA and RIA cases, excepting the VVER case, in this table have been assessed with FRAPTRAN-1.3 and are briefly documented in its release note (FRAPTRAN-1.3, 2005). The remaining cases in the table, including the VVER case, have been assessed using a previous version of the FRAPTRAN code, and are documented in Cunningham et al. (2001b). In total, the number of cases amount to 31. A summary of all these cases is given in table 5.2. In tables 5.1 and 5.2, we have adopted the case classification used by Cunningham & co-workers.

Along with the FRAPTRAN-1.3 code, users can download (at www.pnl.gov) actual input files needed to run the LOCA and RIA cases, excepting the VVER case. The input files for the remaining cases are available in appendix B of code assessment report, Cunningham et al. (2001b). Note that these input files may not be directly executable with FRAPTRAN-1.3, since certain parts of the input format has been modified to the current code version.

The supporting database for the FRAPTRAN code, defined in tables 5.1-5.2, is described briefly in the following sub-sections. Moreover, the materials test MT-4 performed in the Canadian research reactor NRU was executed with the FRAPTRAN-1.3 code to illustrate the output from a LOCA case.

Case/test type	PWR cases	BWR cases	VVER cases *)
LOCA	6	1	0
RIA	13	2	1
Other	2	3	0
Separate effects	0	3	0

*) Fuel rod design used in the Russian VVER reactors

Table 5.1: Spectrum of cases for verification of the FRAPTRAN code.

Comment:
The verification of FRAPTRAN-1.3 should be extended with the aforementioned remaining cases of FRAPTRAN's verification database, table 5.1. The modified fuel thermal conductivity and material properties for mechanical calculations influence the calculated fuel rod behaviour.

Case/Test ID	Rod type	Reactor	Fuel burnup, MWd/kgU	Comments
LOCA /				
MT-1	PWR	NRU	0	11 full-length rods *)
MT-4	PWR	NRU	0	11 full-length rods *)
MT-6A	PWR	NRU	~0	21 full-length rods *)
LOC-11C	PWR	PBF	0	
FRF-2	BWR	TREAT	0	Power ramp, adiabatic heatup
				*) Adiabatic heatup + reflood
RIA /				
Na-1	PWR 17×17	CABRI	63.8	
Na-2	PWR 17×17	CABRI	33	
Na-3	PWR 17×17	CABRI	52.8	
Na-4	PWR 17×17	CABRI	62.3	
Na-5	PWR 17×17	CABRI	64.3	
Na-8	PWR 17×17	CABRI	60	
Na-10	PWR 17×17	CABRI	62	
FK-1	BWR 8×8	NSRR	45	
GK-1	PWR 14×14	NSRR	42.1	
HBO-1	PWR 17×17	NSRR	50.4	
HBO-5	PWR 17×17	NSRR	44	
HBO-6	PWR 17×17	NSRR	49	
MH-3	PWR 14×14	NSRR	38.9	
OI-2	PWR 17×17	NSRR	39.2	
TS-5	BWR 7×7	NSRR	26	
H5T	VVER	IGR	50	
Other /				
FRAP-T6 std problem	PWR	Assumed PWR	0	Hypothetical PWR double-ended cold leg break
IFA-508, rod 11	BWR	HBWR	0	Initial power ascension
IFA-533.2, rod 808R	BWR	HBWR	50	Reinstrumented rod, scram
IE-1, rod 7	PWR-type	PBF	6.8	Power-cooling mismatch
PR-1	BWR-type	PBF	0	Power-cooling mismatch
Separate effects /				
IFA-432, rods 1 & 3	BWR	HBWR	0	Initial power ascension
IFA-513, rod 6	BWR	HBWR	0	Initial power ascension

Table 5.2: Overview of the verification database for the FRAPTRAN code. For references on the cases, see Cunningham et al., (2001b).

Test reactors in table 5.2:

NRU:	National Research Universal reactor, Canada
PBF:	U.S. Power Burst Facility
TREAT:	U.S. Transient Reactor Test Facility
CABRI:	Cadarache, France
NSRR:	Nuclear Safety Research Reactor, Japan
IGR:	Impulse Graphite Reactor, Russia
HBWR:	Halden heavy-water BWR, Norway

5.1 Loss-of-coolant accident

The fuel rod behaviour under LOCA has been assessed by FRAPTRAN for five different LOCA experiments performed in three different test reactors (Cunningham et al., 2001b; FRAPTRAN-1.3, 2005). Three of the LOCA tests were carried out in the Canadian National Research Universal (NRU) reactor at Chalk river and the two remaining tests in the Power Burst Facility (PBF) and Transient Reactor Test Facility (TREAT).

The parameters used in the assessment of the code performance are:

- Time to rupture
- Axial location of rupture and ballooning (rupture hoop strain)
- Cladding axial strain history
- Rod gas pressure history

The LOCA experiments utilized for the verification of FRAPTRAN are summarized in table 5.3, followed by short descriptions. In addition to these experiments, a series of LOCA tests performed in the French PHEBUS facility are also briefly mentioned at the end of this section. These results from PHEBUS were assessed by an earlier development of the FRAPTRAN code, i.e. FRAP-T.

	MT-1	MT-4	MT-6A	LOC-11C	FRF-2
Test reactor	NRU	NRU	NRU	PBF	TREAT
Date of test	April 1981	May 1982	May 1984	...	...
No. of rods in bundle	11	12	21	4	7
Source	1)	2)	3)	4)	5)
Rod design /					
Cladding material	Zr-4	Zr-4	Zr-4	Zr-4	Zr-4
Cladding OD, mm	9.63	9.63	9.63	10.72	14.31
Cladding ID, mm	8.41	8.41	8.41	9.50	12.68
Pellet diameter, mm	8.26	8.26	8.26	9.29	12.56
Active fuel length, mm	3658	3660	3660	915.5	609.6
Total rod length, mm	3850	3850	3850	1003	685.8
Rod pitch, mm	12.75	12.75	12.75	...	...
Plenum volume, cm^3	13.62	13.62	13.62	3.29	7.19
He gas pressure, MPa	3.2	4.62	6.03	b)	0.52
Fuel enrichment, %U-235	3	2.93	2.93	9.6	1.5
Fuel density, %TD	95	95	95	95	95
Test results /					
Time to rupture, s	60-95	52-58	58-64	...c)	30-35
No. of ruptured rods	6	12	21	0	7
Axial location of rupture d), mm	2000	2680	NM	...	≈350
Av. rupture hoop strain, %	43	72	NM a)	...	35-50
Peak clad temperature, K	1148	1459	≈1175	≈1030	≈1600
Av. rupture temperature, K	1145	1094	1050-1140	...	1470-1600

OD = Outer Diameter, ID = Inner Diameter, TD = Theoretical Density, NM = Not Measured

a) Strain value was not measured, but visual inspection revealed that rupture strain was “large”.

b) 2 rods at 0.103 MPa (rods 1 and 4), 1 rod at 2.41 MPa (rod 3) and 1 rod at 4.82 MPa (rod 2).

c) The two rods with the highest fill pressures (rods 2 and 3) experienced clad ballooning.

d) From bottom end of fuel column.

1) Russcher et al., 1981 2) Cunningham et al., 2001b & refs. therein
3) Wilson et al., 1993 4) Buckland et al., 1978; Larson et al., 1979
5) Lorenz & Parker, 1972

Table 5.3: Summary of simulated in-reactor LOCA tests assessed by the FRAPTRAN 1.3 code.

5.1.1 NRU tests

The objective of the NRU series of tests was to perform simulated LOCA experiments using full-length PWR fuel rods to study cladding deformation, flow blockage and fuel rod coolability. The tests assemblies in the three NRU tests MT-1, MT-4 and MT-6A comprised arrays of 11, 12 and 21 fuel rods, respectively.

The NRU tests were conducted on initially unirradiated rods with Zircaloy-4 cladding. Some key characteristics of these rods and simulated LOCA test results are shown in table 5.3. The NRU reactor has a coolant inlet temperature of 37°C at system pressure of 0.65 MPa. Three phases of a LOCA, i.e. heat-up, reflood and quench were performed in test reactor environment to consider the low-level decay power during a LOCA after shutdown.

MT-1:
The rods in the MT-1 test were subjected to adiabatic heat-up followed by reflood. More specifically, the *preconditioning phase* for the MT-1 test was performed at fuel rod average power of 18.7 kW/m and water cooling at a pressure of 8.62 MPa. The *pretransient phase* was conducted with steam cooling at a mass flow rate of 0.378 kg/s and an average fuel rod power of 1.24 kW/m. Finally, in the *transient phase* the test assembly was subject to adiabatic heat-up in stagnant steam. The steam flow was shut off after 10 s and reflooding, at a rate of 0.051 m/s, was initiated after 32 s. The reflooding rate is the rate of increase of the water level in the test section per unit time. Peak cladding temperatures of up to 1172 K were targeted in the MT-1 test to obtain clad rupture in the high α to (α+β)-phase of the material. The main results from the MT-1 test are summarized in table 5.3.

MT-4:
The aim of the MT-4 test was similar to that of MT-1. However, the prime objectives of the MT-4 test were (i) to provide enough time in the temperature range for α-Zircaloy (1033 to 1200 K) to produce ballooning and eventually burst of all the 12 test fuel rods before initiation of reflooding, (ii) to obtain heat transfer coefficients for ballooned and ruptured rods and (iii) to measure fuel rod internal gas pressure during the test, i.e. under progressing rod deformation.

The preconditioning phase of the MT-4 test was conducted with water coolant pressure of 8.27 MPa and a mass flow rate of 16.3 kg/s. Furthermore, the precondition comprised also of two power increases to allow fuel pellets to crack and relocate. The heat-up rate in the transient phase was around 8.3 K/s and lasted for about 1.5 minutes. Reflood in the test was initiated after 57 s with different flooding rates. Some key results from the MT-4 test are summarized in table 5.3.

MT-4, description of case input & output:
The MT-4 LOCA test was run as a sample case with FRAPTRAN-1.3 and some of the key results are plotted in the sequel. A selection of other results from this sample case is given in appendix B. The active length of the rod in the analysis is divided into 12 equally long axial segments and clad burst is calculated to occur in segment number 8 (numbering starting from bottom end of rod). The average clad temperature variation with time calculated in the burst segment is shown in figure 5.1. The average clad temperature attains its maximum of about 1170 K at 80 s after initiation of the event. At rupture, i.e. at 60 s, the average clad temperature is calculated to be about 1073 K, which is very close to the measured value of 1094 K, see table 5.3. The peak clad temperature measured in the MT-4 test amounts to 1459 K (1186°C). However, the peak clad temperature due to circumferential temperature variation was not available for comparison from this FRAPTRAN run.

The equivalent fractions of clad wall reacted (ECR) calculated by the Baker-Just and Cathcart-Pawel high-temperature oxidation models available in the FRAPTRAN-1.3 code are depicted as a function of time in figure 5.2. The maximum ECR values calculated for the MT-4 test are below 1.1%.

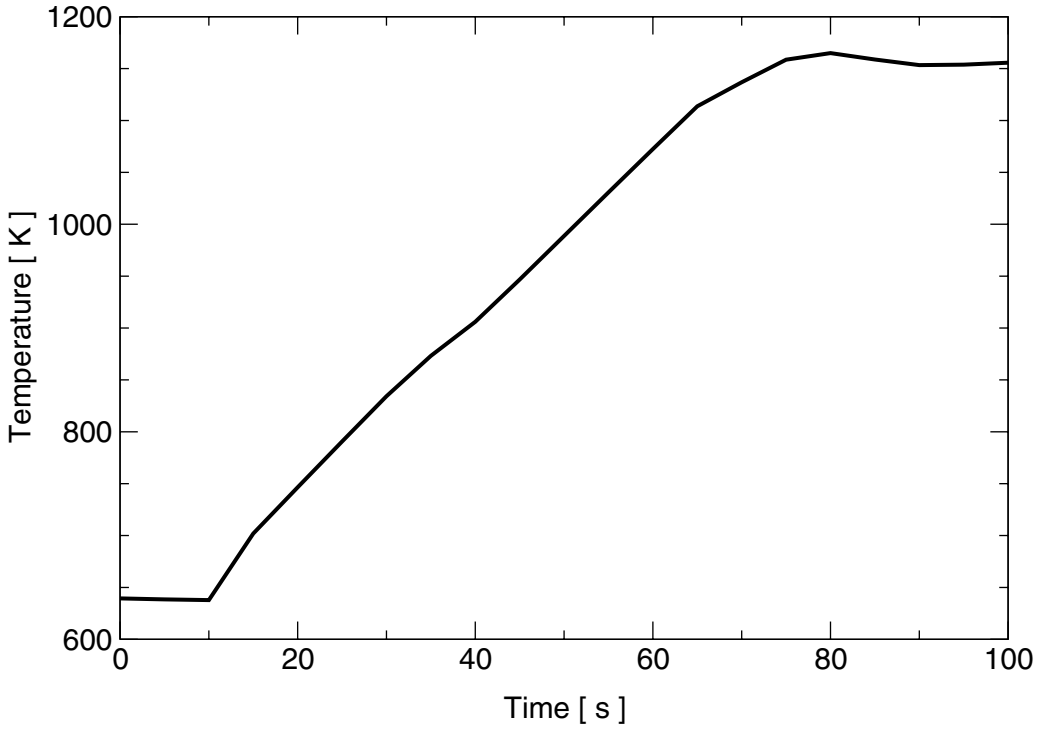

Figure 5.1: Calculated average clad temperature in axial segment 8, where rod burst is retrodicted by FRAPTRAN-1.3. The axial elevation of the burst node is 2.286 m.

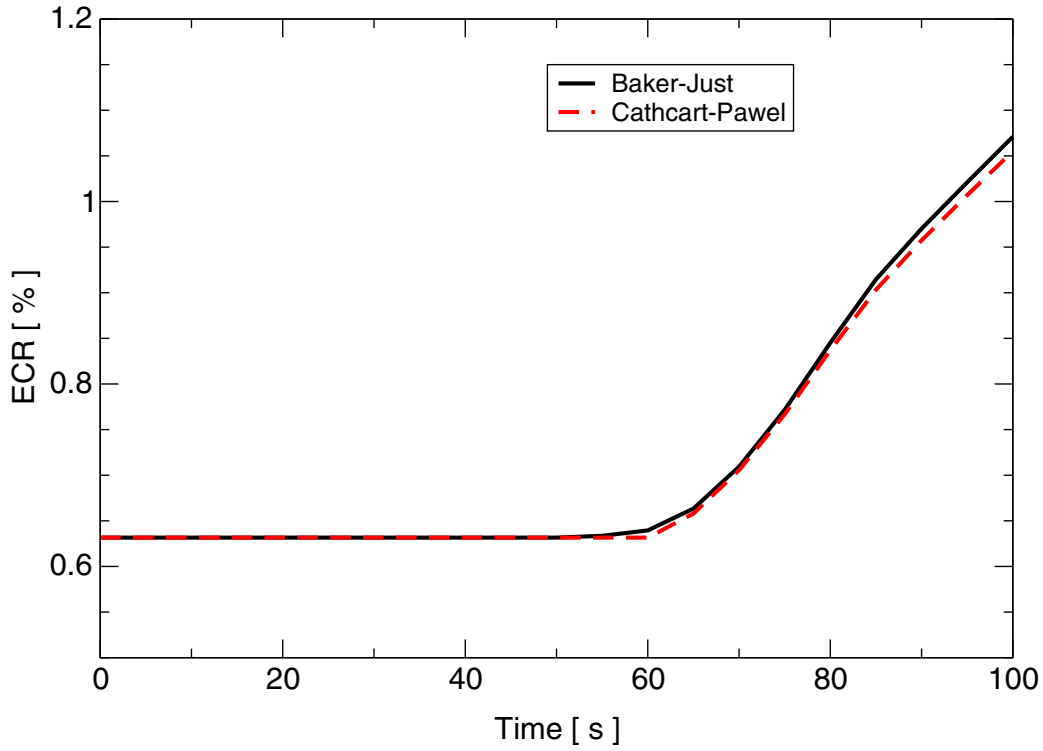

Figure 5.2: Calculated fraction of clad wall reacted in the MT-4 LOCA test. The equivalent cladding reacted (ECR) is determined by using the Baker-Just and Cathcart-Pawel high-temperature oxidation models implemented in the FRAPTRAN-1.3 code. The results pertain to axial segment 8.

MT-6A:
A principal difference between the MT-6A test and the previous tests is the redesign of the test configuration (test train) to reduce cladding circumferential temperature gradients thus enhancing uniform ballooning and the associated flow blockage. A total of 21 rods were used in the MT-6A test, whereof nine had been used in a previous test (MT-3), which are not included in the FRAPTRAN verification database. Due to an error in the computer controlling the test, the system pressure during the heat-up phase was 1.72 MPa instead of 0.28 MPa, i.e. about six times higher than the target system pressure. In addition, the desired temperature control was not achieved. However, the cladding inner surface temperature and rod internal gas pressure variations measured in this test are evaluated. Key results from the test are given in table 5.3. For further details on this test, see Cunningham et al. (2001b) and references therein.

5.1.2 PBF test: LOC-11C

In the LOC-11 test series, four PWR-type, unirradiated fuel rods were subjected to cladding temperatures similar to those expected for the highest powered PWR rods during blowdown and heat-up of a 200% double-ended cold leg break. The test sequence was heat-up, power calibration, pre-conditioning, decay heat build-up, blowdown and quench, and cool down. Three sequential tests were performed, LOC-11A, LOC-11B and LOC-11C. There was no indication of fuel rod failure in any of the three tests. The target peak cladding temperature in the LOC-11C test, which is utilized in the FRAPTRAN verification, was 1030 K.

The LOC-11C test comprises four fuel rods with identical design except for the helium fill gas pressures, whereof two were pre-pressurized to 0.103 MPa (rods 1 and 4) and the other two to 2.41 MPa (rod 3) and 4.82 MPa (rod 2). Hence, this test provides three computational cases for code verification. Some key results from the test are summarized in table 5.3. For further details on this test, see Cunningham et al. (2001b) and references therein.

5.1.3 TREAT test: FRF-2

The fuel rod failure test, FRF-2, comprised a fresh seven-rod bundle irradiated in the U.S. transient reactor test facility (TREAT). The design of the test rods is summarized in table 5.3. In order to achieve the target peak cladding temperature of approximately 1600 K in the test, rod average power levels up to about 36 kW/m were induced during the transient. The rods ruptured between 30 and 35 s after initiation of the test, at cladding temperatures ranging from 1470 to 1600 K. The test results are briefly given in table 5.3, however, for details regarding the test consult the FRAPTRAN assessment in Cunningham et al. (2001b) and references therein.

Comment:
Note that, FRF-2 is considered to be a BWR case in the FRAPTRAN documentation although it is stated that the rods have Zircaloy-4 cladding, Cunningham et al. (2001b).

5.1.4 PHEBUS tests

Earlier developments of the FRAPTRAN code, i.e. FRAP-T, were verified against integral in-pile LOCA experiments performed in the PHEBUS facility in France (Réocreux & Scott de Martinville, 1990). The PHEBUS series of LOCA experiments in their work were conducted in the 1980s and involved PWR-type test assemblies with 25 fuel rods (5×5 array). The length of the rods used was 1 m and the heated length 0.8 m. More specifically, the investigators explored the modelling capability of a number of computer codes, one of them being FRAP-T, by comparing calculations with results from the PHEBUS experiments. The parameters covered in their work comprised (i) burst time, (ii) cladding burst temperature, (iii) rod internal pressure and (iv) cladding burst strain. Among the PHEBUS LOCA experiments performed, the test 218 has been used for comparison of the predictive capability of various fuel rod codes (Scott de Martinville & Pignard, 1987). The PHEBUS test 218 is also termed International Standard Problem No. 19 (ISP-19).

Comment:
The PHEBUS LOCA tests are not part of the assessment database for FRAPTRAN-1.3. Unfortunately, the article by Réocreux & Scott de Martinville (1990) is insufficient for an independent review of their results, since it lacks crucial data needed for modelling, and as far as we know, they have not published any further details on this particular investigation. However, the OECD/NEA code comparison report by Scott de Martinville & Pignard (1987) contains suitable information on PHEBUS test 218 for assessment of FRAPTRAN-1.3.

5.2 Reactivity initiated accident

The reactivity initiated accident (RIA) assessment database of the FRAPTRAN-1.3 code consists of 7 tests from the ongoing RIA test program in the French CABRI reactor (REP Na series) and 8 RIA tests carried out in the Japanese Nuclear Safety Research Reactor (NSRR). The particular tests used for RIA assessment of FRAPTRAN-1.3 are listed in table 5.4, and are available as input files via the internet at www.pnl.gov/frapcon3. The database covers burnups up to 64 MWd/kgU. Some of these tests are briefly described in Cunningham et al. (2001b). Further details on these RIA tests may be found in Jernkvist et al. (2004). We note that the supporting database for FRAPTRAN previously also included a RIA test (IGR-H5T) performed in the Russian IGR research reactor (Cunningham et al., 2001b). The VVER-type rodlet in this test had a burnup of 50 MWd/kgU and was subjected to a power pulse with large width (840 ms) and a peak fuel enthalpy of 176 cal/g (Yegorova et al., 1999). The rod was equipped with Zr-1%Nb cladding material. The rod failed in the test.

Test ID	Design *)	Fuel burnup MWd/kgU	Pulse width ms	Peak fuel enthalpy J/g	Failure enthalpy J/g
Na-1	17×17	63.8	9.5	460	126
Na-2	17×17	33	9.1	882	Survived
Na-3	17×17	52.8	9.5	502	Survived
Na-4	17×17	62.3	75	404	Survived
Na-5	17×17	64.3	9.5	439	Survived
Na-8	17×17	60	75	443	343
Na-10	17×17	62	31	461	331
FK-1	8×8	45	4.4	544	Survived
GK-1	14×14	42.1	4.6	389	Survived
HBO-1	17×17	50.4	4.4	306	251
HBO-5	17×17	44	4.4	334	322
HBO-6	17×17	49	4.4	356	Survived
MH-3	14×14	38.9	4.4	281	Survived
OI-2	17×17	39.2	4.4	453	Survived
TS-5	7×7	26	4.5	410	Survived

*) The 7×7 and 8×8 arrays represent BWR designs and the rest PWR designs.

Table 5.4: RIA assessment database of the FRAPTRAN-1.3 code.

The most recent assessment of the RIA capability of FRAPTRAN is that reported by Geelhood and co-workers (2004). In that work, they compare calculated fuel enthalpies (at failure and maximum) and permanent hoop strains of the rods with measured values. In addition, they compare the predictability of the failure model in FRAPTRAN for the RIA cases. An assessment of the RIA database is also provided in the FRAPTRAN-1.3 release document, FRAPTRAN-1.3 (2005).

Comment:
Geelhood & company (2004) used a version of FRAPTRAN with three "new" models in their analysis of the RIA data. The modifications referred in their work pertain (i) the fuel thermal expansion model, (ii) the clad yield stress correlation and (iii) the clad low-temperature failure model (termed uniform elongation model in their paper). We note that the fuel thermal expansion model mentioned by Geelhood et al. (2004) is not included in FRAPTRAN-1.3. In addition, the cladding yield stress correlation given by Geelhood differs from that given in the FRAPTRAN-1.3 release document (FRAPTRAN-1.3, 2005).

5.3 Other cases

Other cases used for the code verification described by Cunningham et al. (2001b) comprise

- FRAP-T6 standard problem
- Halden IFA-508, rod 11
- Halden IFA-533.2, Rod 808R
- PBF IE, rod 7
- PBF PR-1

5.3.1 FRAP-T6 standard problem

The FRAP-T6 standard problem comprises a constructed transient case for a hypothetical PWR double-ended cold leg break, and was included in the documentation when FRAP-T6 was issued in 1981. Unirradiated fuel was assumed in the case. The aim of the case was to illustrate possible changes in FRAPTRAN since FRAP-T6 was first issued. For further details, see Cunningham et al. (2001b).

5.3.2 Halden IFA-508, rod 11

The assessment of the FRAPTRAN's capability to predict fuel rod axial deformations under pellet-cladding mechanical interaction (PCMI) is performed by utilizing data from the IFA-508 experiment conducted in the Halden heavy-water BWR (HBWR) in Norway. The test rig, equipped with fresh fuel rods, was subject to a 30 hour long power cycle consisting of a power rise to high power followed by a power reduction to zero power. The particular rod (rod 11) in the test rig used for FRAPTRAN assessment experienced a peak power of about 47 kW/m. The power increase in the test was performed in a step-wise manner with certain hold times between the steps. The rod was instrumented with a fuel centreline thermocouple and cladding axial strain sensor.

It was observed that the axial length of the rod under PCMI decreased during the hold periods at constant power (Cunningham et al., 2001b). According to Cunningham and co-workers the relaxation effect of axial PCMI is not calculated by FRAPTRAN since the code lacks a fuel relaxation model. However, the onset of PCMI in the experiment is captured well by FRAPTRAN, but the subsequent development of axial pellet-clad contact forces are strongly overestimated (Cunningham et al., 2001b).

Comment:
The disparity seen between measured and calculated axial deformations is not only attributed to the absence of a fuel relaxation model in FRAPTRAN, but also to simplistic modelling of pellet-cladding contact in the code. The basis for pellet-cladding contact modelling in FRAPTRAN is the same as in FRAPCON-3, see Jernkvist & Massih (2002) for an outline of the model. Moreover, the cladding creep properties play also an important role in fuel rod strain relaxation behaviour.

5.3.3 Halden IFA-533.2, rod 808R

The Halden experiment IFA-533.2 is used to demonstrate FRAPTRAN's capability to calculate fuel centreline temperature under transient conditions. The test rig for the IFA-533.2 irradiation comprised rods that had been pre-irradiated in the IFA-409 experiment and then re-instrumented with centreline thermocouples. A key feature of the IFA-533.2 irradiation is the periodic scrams exercised after certain burnup steps and the online measurement of transient centreline temperature during the scrams. The temperature data from the experiment are suitable for assessment of fuel performance changes with burnup. More specifically, the temperature data for assessment of the transient fuel temperature behaviour of FRAPTRAN was taken from rod number 808R at burnup of 50 MWd/kgU. The outcome from the assessment performed by Cunningham et al. (2001b) shows that FRAPTRAN overestimates the fuel time constant for this sample case, for details see Cunningham et al. (2001b).

5.3.4 PBF IE-1, rod 7

The PBF IE-1 test involved pre-irradiated PWR rods that were subject to a variety of power and coolant conditions, i.e. to *power-cooling mismatch* (Cunningham et al., 2001b). During the sixth cycle of the test the rods were brought to power, kept at that power while the coolant mass flow was decreased until the rods experienced departure from nucleate boiling. Cunningham and co-workers used the cladding axial strain data measured for rod 7 from this experiment to show the behaviour calculated by FRAPTRAN. The rod average burnup of this particular rod was 6.8 MWd/kgU.

The FRAPTRAN results reported by Cunningham show that the axial cladding strain during increase to power is in fair agreement with measurement but the succeeding behaviour is not at all captured. FRAPTRAN is not capable to calculate the onset of DNB correctly in this experiment. The authors recommend users of FRAPTRAN to use clad-to-coolant heat transfer data from a thermo-hydraulics code instead of using the built-in coolant channel model.

5.3.5 PBF PR-1

The PBF PR-1 test subjected four unirradiated BWR-type fuel rods to a variety of power coolant conditions, including some RIA-type conditions at the end of the test series. During cycle 17 of this test the rods were held at a constant power of about 34 kW/m while the coolant mass flow was reduced. Fuel centreline and cladding temperatures, cladding axial strain and rod internal gas pressure were measured in the test and are used for verification of the FRAPTRAN code (Cunningham et al., 2001b). One of the four rods failed in the test.

5.4 Separate effects tests

The tests termed as “separate effects tests” by Cunningham & co-workers (2001b) comprise three fuel rods from two irradiation experiments performed in the Halden reactor, namely the IFA-432 and IFA-513 tests. These tests used well-characterised, fresh BWR-type fuel rods which were instrumented with fuel centreline thermocouples, gas pressure sensors and cladding axial strain sensors. Fuel centreline and cladding axial strain data obtained as a function of rod linear power are used for verification of FRAPTRAN. Since the power increase is slow in these experiments, they are also included in fuel centreline temperature verification of the FRAPCON-3 code (Berna et al., 1997; Jernkvist & Massih, 2002).

6 Concluding remarks

In this report, we have evaluated the FRAPTRAN-1.3 computer code with respect to its applicability, modelling capability, user friendliness and supporting experimental database. In the evaluation, we have primarily focused on the code's capacity for calculation of fuel rod behaviour under LOCA conditions. We conclude that FRAPTRAN-1.3 is applicable to thermo-mechanical analyses of both BWR and PWR fuel rods under transient operational conditions. However, since its material models have been developed for Zircaloy material, these are not directly applicable for other zirconium-based cladding alloys other than Zircaloy. The applicability of the current version as a self-standing analysis tool for LOCA and RIA analyses depends highly on the numerical robustness of the coolant channel model for generation of clad-to-coolant heat transfer boundary conditions.

Based on our evaluation, to improve the capability of FRAPTRAN-1.3 for LOCA calculations, we suggest the following efforts:

1) According to the developers of the FRAPTRAN-1.3 code, the coolant channel model option to calculate clad-to-coolant heat transfer conditions is not recommended for LOCA and RIA simulations. They refer to numerical problems in the code. This shortcoming should be investigated and actions should be taken to eliminate or at least to alleviate its causes.

2) The burst behaviour calculated by the BALON2 model should be verified with relevant experiments in which burst strain as a function of burst temperature has been measured. The burst strain as a function of burst temperature from LOCA experiments at a given heating rate shows a double-peaked behaviour with a minimum in the (α+β)-phase region. The verification should cover several heat rates up to about 100 Ks^{-1}.

3) The verification of FRAPTRAN-1.3's BALON2 module regarding the effect of burst strain on circumferential temperature variation is very limited, both concerning the heat rates and the temperature ranges covered. This verification should be extended to heat rates up to at least 100 Ks^{-1}, and should also cover at a least the burst behaviour in the (α+β) and β phase regions.

4) The burst stress criterion in BALON2 is a function of temperature and the strength coefficient for fully annealed Zircaloy cladding. The validity of this failure model should also be verified for cold-worked and recrystallization annealed cladding materials.

5) The strain hardening for irradiated Zircaloy material seems to be overestimated in the stress-strain curves calculated by the material properties model. The material properties model in FRAPTRAN should be subject to a general review.

6) The cladding model should be extended to account for different creep rates in the α, (α+β) and β phase regions of the material. To achieve this, a number of models need to be extended, and non-existing models developed. Introducing this capability, may need reformulation of the treatment of creep deformation in FRAPTRAN. Hence, the subtasks defined in the sequel should be preceded by a feasibility study.

6a) A model calculating the fraction of cladding wall in the respective phase regions under transient conditions should be developed and included. This requires a formulation that takes into account the kinetics of the phase transformations, i.e. from $\alpha \rightarrow \beta$ and $\beta \rightarrow \alpha$. The model should include the behaviour of Zircaloy and Zr-Nb cladding materials.

6b) The models, in item 6a) above, should be further extended to consider the effect of oxidation and hydrogen pickup on the phase transformations and associated kinetics. The presence of oxygen and hydrogen in Zr matrix lowers the $\alpha \rightarrow \beta$ transformation temperature, thereby promoting cladding creep deformation.

6c) After completing the above items (6 and 6a-b), the pertinent models should be included in FRAPTRAN and verified with relevant experimental data discussed in the complementary report (Massih, 2007).

7) The clad high-temperature oxidation seems to be underestimated by the FRAPTRAN code. The oxide layer thickness calculated by FRAPTRAN (checked by NRU MT-4 case) does not match that of Baker-Just relation. The implementation of clad inside and outside high-temperature oxidation correlations should be scrutinized and corrected. The oxide calculation constitutes the basis for the ECR calculation.

8) The international standard problem ISP-19 (PHEBUS test 218), which has in the past been used for LOCA assessment of fuel rod codes (inter alia different versions of FRAP-T), should be reassessed with the FRAPTRAN-1.3 code.

7 References

Allison, C.M., Berna, G.A., Chambers, R., Coryell, E.W., et al., 1993.
SCDAP/RELAP5/MOD3.1 Code Manual Volume IV: MATPRO – A library of materials properties for light-water-reactor accident analysis,
US NRC Report NUREG/CR-6150 (EGG-2720), Volume IV.

Berna, G.A., Beyer, C.E., Davis, K.L., Lanning, D.D., 1997.
FRAPCON-3: A computer code for the calculation of steady-state, thermal-mechanical behavior of oxide fuel rods for high burnup,
US NRC Report NUREG/CR-6534, Volume 2.

Bohn, M.P., 1977.
FRACAS: A subcode for the analysis of fuel pellet-cladding mechanical interaction,
Report TREE-NUREG-1028.

Buckland, J.B., Coppin, C.E., White, C.E., 1978.
Experiment data report for PBF-LOCA tests LOC-11B and 11C,
US NRC Report NUREG/CR-0303 (TREE-1232), Washington D.C.

Cazalis, B., Bernaudat, C., Yvon, P., Desquines, J., Poussard, C., Averty, X., 2005.
The PROMETRA program: A reliable material database for highly irradiated Zircaloy-4, ZIRLO and M5 fuel claddings,
Proc. 18th International Conference on Structural Mechanics in Reactor Technology (SMiRT 18), Beijing, China, August 7-12, 2005.

Cunningham, M., Beyer, C.E., Medvedev, P.G., Berna, G.A., 2001a.
FRAPTRAN: A computer code for the transient analysis of oxide fuel rods,
US NRC Report NUREG/CR-6739 (PNNL-13576), Volume 1, August 2001.

Cunningham, M., Beyer, C.E., Panisko, F.E., Medvedev, P.G., et al., 2001b.
FRAPTRAN: Integral assessment,
US NRC Report NUREG/CR-6739 (PNNL-13576), Volume 2, August 2001.

Desquines, J., Cazalis, B., Bernaudat, C., Poussard, C., Averty, X., Yvon, P., 2005.
Mechanical properties of Zircaloy-4 PWR fuel cladding with burnup 54-64 MWd/kgU and implications for RIA behaviour,
J. ASTM Intern., Vol.2, No. 6, June 2005.

Erbacher, F.J., Leistikow, S., 1987.
Zircaloy fuel cladding behavior in a loss-of-coolant accident,
Zirconium in the Nuclear Industry, 7th International Symposium, Adamson, R.B., Van Swam, L.F.P. (Eds), ASTM STP 939, American Society for Testing and Materials, Philadelphia, PA, USA, 451-488.

Federici, E., Lamare, F., Bessiron, V., Papin, J., 2000.
Status of development of the SCANAIR code for description of fuel behavior under reactivity initiated accidents,
Proc. 2000 Int. Topical Meeting on LWR Fuel Performance, Park City, Utah, USA, April 10-13, 2000.

Ferner, J., Rosinger, H.E., 1985.
The effect of circumferential temperature variation on fuel cladding failure,
J. Nucl. Mater. 132, 167-172.

FRAPTRAN-1.3, 2005.
FRAPTRAN-1.3 Release Document, August 2005,
Available for FRAPCON-3/FRAPTRAN users via the internet at www.pnl.gov/frapcon3.

Geelhood, K.J., Beyer C.E., Cunningham M.E., 2004.
Modifications to FRAPTRAN to predict fuel rod failures due to PCMI during RIA-type accidents,
Proc. International Meeting on LWR Fuel Performance, Orlando, Florida, USA, September 19-22, 2004.

Hagrman, D.L., 1981.
Zircaloy cladding shape at failure (BALON2),
EGG-CDAP-5379, EG&G Idaho, Inc., Idaho Falls, Idaho.

Hill, R., 1948.
A theory of the yielding and plastic flow of anistropic solids,
Proc. Royal Society of London, Series A, Mathematical and Physical Sciences 193, 281-297.

Hult, J., 1968.
Hållfasthetslära,
Almqvist & Wiksells boktryckeri AB, Andra upplagan, Uppsala, (In Swedish).

Jernkvist, L.O., Limbäck, M., 1995.
Analysis of fuel rod behaviour under LOCA using the STAV-T fuel performance code,
Proc. 13th International Conference on Structural Mechanics in Reactor Technology (SMiRT 13), Porto Alegre, Brazil, August 13-18, 1995.

Jernkvist, L.O., Massih, A., 2002.
Evaluation of the FRAPCON-3 computer code,
Swedish Nuclear Power Inspectorate (SKI) Research Report 02:29, Stockholm, Sweden.

Jernkvist, L.O., Massih, A.R., Rudling, P., 2004.
A strain-based clad failure criterion for reactivity initiated accidents in light water reactors,
Swedish Nuclear Power Inspectorate (SKI) Research Report 2004:32, Stockholm, Sweden.

Jernkvist, L.O., Massih, A.R., 2005.
Models for rod behaviour at high burnup,
Swedish Nuclear Power Inspectorate (SKI) Research Report 2005:41, Stockholm, Sweden.

Larson, J.R., Spore, J.W., McCardell, R.K., Broughton, J.M., Sepold, L.K., 1979.
PBF-LOCA test series test LOC-11 test result report,
US NRC Report NUREG/CR-06183 (TREE-1329), Washington D.C.

Limbäck, M., Jernkvist, L.O., Andersson, T., 1998.
Deformation and rupture of Zr-based tubes at high temperatures,
SFMT Conference on High Temperature Materials, Sigtuna, Sweden, April 28-29, 1998.

Lorenz, R.A., Parker, G.W., 1972.
Final report on the second fuel rod failure transient test of a Zircaloy-clad fuel rod cluster in TREAT,
ORNL-4710, Pacific Oak Ridge National Laboratory, Oak Ridge, Tennessee.

Massih, A.R., 2007.
Review of experimental data for modelling LWR fuel cladding behaviour under loss of coolant accident conditions,
Quantum Technologies Technical Report TR06-006.

Ohira, K., Itagaki, N., 1997.
Thermal conductivity measurements of high burnup UO_2 pellet and a benchmark calculation of fuel center temperature,
Proc. ANS Topical Meeting on LWR Fuel Performance, Portland, Oregon, March 2-6, 1997.

Pawel, R.E., Perkins, R.A., McKee, R.A., Cathcart, J.V., et al., 1977.
Diffusion of oxygen in beta-Zircaloy and the high temperature Zircaloy steam reaction,
Zirconium in the Nuclear Industry: ASTM STP 633, American Society for Testing and Materials, pp 119-133.

Pawel, R.E., Cathcart, J.V., McKee, R.A., 1980.
"Anomalous" oxide growth during transient-temperature oxidation of Zircaloy-4,
Oxidation of Metals 14, 1-13.

RELAP5, 2001.
RELAP5-3D code manual, volume 1: Code structure, system models and solution methods,
INEEL Report INEEL-EXT-98-00834, revision 1.3a, Idaho Falls.

Réocreux, M., Scott de Martinville, E.F., 1990.
A study of fuel behavior in PWR design basis accident: an analysis of results from the PHEBUS and EDGAR experiments,
Nucl. Engin. & Design 124, 363-378.

Rosinger, H.E., 1984.
A model to predict the failure of Zircaloy-4 fuel sheathing during postulated LOCA conditions,
J. Nucl. Mater. 120, 41-54.

Russcher, G.E., Marshall, R.K., Hesson, G.M., Wildung, N.J., Rausch, W.N., 1981.
LOCA simulation in the NRU reactor: materials test 1,
U.S. Nuclear Regulatory Commission report NUREG/CR-2152-V1 (PNL-3835),
Washington D.C.

Scott de Martinville, E., Pignard, M., 1987.
International Standard Problem ISP-19, Behavior of a fuel rod bundle during a large break LOCA transient with two peaks temperature history (PHEBUS experiment); FINAL COMPARISON REPORT,
OECD/NEA CSNI Report 131.

Siefken, L.J., Allison, C.M., Bohn, M.P., Peck, S.O., 1981.
FRAP-T6: A computer code for the transient analysis of oxide fuel rods,
US NRC Report NUREG/CR-2148 (EGG-2104), EG&G Idaho, Inc., Idaho Falls.

Uchida, M., 1984.
Application of a two-dimensional ballooning model to out-pile and in-pile simulation experiments,
Nucl. Engin. & Design 77, 37-47.

Yegorova, L., Schmitz, F., Papin, J., 1999.
Mechanical behaviour of fuel element during RIA transients,
Proc. EUROSAFE-1999 Meeting, November18-19, Paris, 1999.

Wilson, C.L., Hesson, G.M., Pilger, J.P., King, L.L., Panisko, F.E., 1993.
Large-break LOCA, in-reactor fuel bundle materials test MT-6A,
PNL-8829, Pacific Northwest Laboratory, Richland, Washington.

Appendix A: FRAPTRAN-1.3 clad mechanical properties model

The model for cladding mechanical properties in FRAPTRAN-1.3 is based on MATPRO handbook (Allision et al., 1993) and a new set of coefficients has been developed for Zircaloy-2 and Zircaloy-4 cladding materials (FRAPTRAN-1.3, 2005). The new model is based on PNNL's material property tests (PNNL database) and irradiated cladding tube samples of stress-relieved annealed (SRA) Zircaloy-4 tested in the PROMETRA program (Desquines et al., 2005). The PNNL database is not described in the FRAPTRAN documentation, thus thermo-mechanical treatment as well as other properties of the specimens used in these tests are unknown to us. In the model, the elastic part of its stress-strain (σ, ε) behaviour is described by Hooke's law ($\sigma = E\varepsilon$, E is Young's modulus) and the plastic (post-yield) strain behaviour with a power law relationship of the form

$$\sigma = K\varepsilon^n \left(\frac{\dot{\varepsilon}}{10^{-3}} \right)^m , \qquad \text{(A1)}$$

where K is the strength coefficient in Pa, $\dot{\varepsilon}$ the strain rate in s^{-1}, n the strain hardening exponent and m the strain rate sensitivity exponent. Both these exponents are dimensionless. Calculated tress-strain curves for irradiated Zircaloy-4 at constant strain rate of 0.005 s^{-1} and at temperatures (T) of 623, 1000 and 1200 K are plotted in figure A1. The fast neutron fluence Φ (>1 MeV), amount of cold-work (CW) and oxygen content in cladding material was set to 10×10^{25} m^{-2}, 0% and 1200 ppm, respectively. The oxygen content influences Young's modulus and the coefficients of eq. (A2) by enhancement functions. For oxygen dependencies in the model, see MATPRO (Allison et al., 1993).

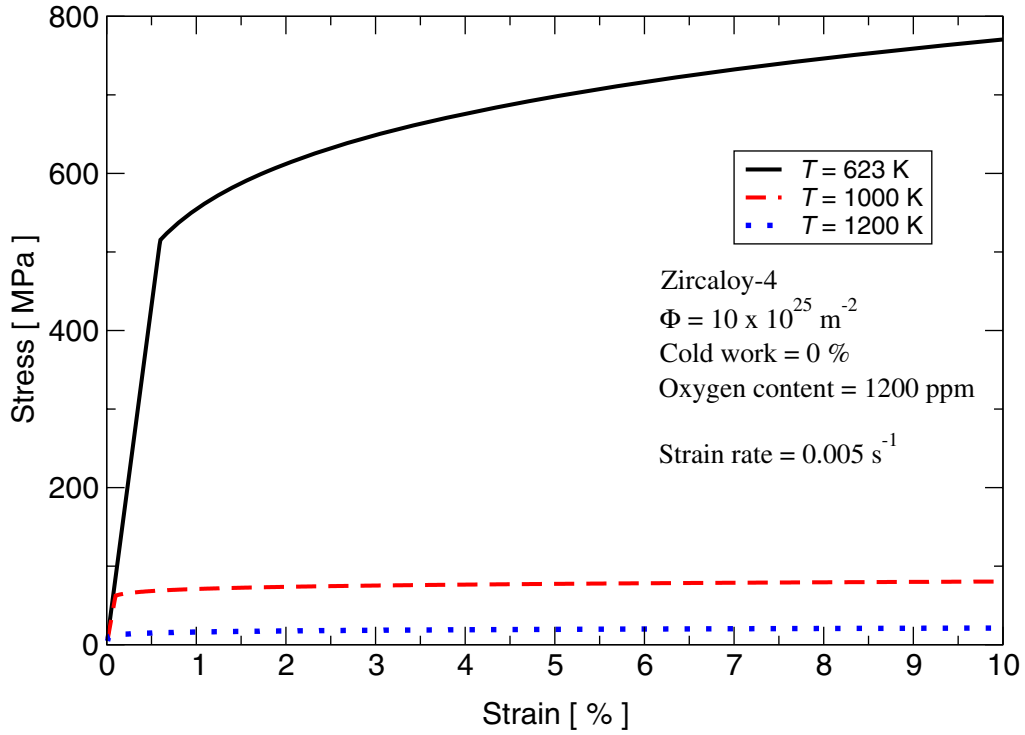

Figure A1: Calculated stress-strain curves for irradiated Zircaloy-4 at temperatures of 623, 1000 and 1200 K.

The expressions for the various coefficients in equation (A1), as implemented in the FRAPTRAN-1.3 code, are given in the sequel. Differences relative to MATPRO are plotted in figures for comparison. The temperature range from 1090 to 1255 K corresponds to the mixed (α+β) phase region for Zircaloy and above 1255 K for the β phase region.

The strength coefficient K in equation (A2) is a function of temperature, cold-work, fast neutron fluence and cladding type (Zircaloy-4 or Zircaloy-2). The magnitude of temperature-dependent part of the strength coefficient, $K_1(T)$, in this equation is plotted in figure A2. In figure A3, the irradiation enhancement factor $K_3(\Phi)$ of the strength coefficient used in FRAPTRAN-1.3 is compared with that of MATPRO. The strain rate exponents applied in FRAPTRAN-1.3 and that defined in MATPRO are plotted as a function of temperature in figure A4. Note that the strain rate exponent in MATPRO is strain rate dependent in the (α+β) phase temperature range for strain rates exceeding 6.34×10^{-3} s^{-1}. The strain hardening exponent n in equation (A8) is a function of temperature and fast neutron fluence. The temperature dependency of strain hardening exponent $n_1(T)$ in this equation is plotted in figure A5 and the irradiation-dependent part $n_2(\Phi)$ in figure A6. Note that the irradiation part of the strain hardening exponent in MATPRO is also dependent on cold-work.

The strength coefficient:

$$K = K_1(T)\frac{1+K_2(CW)+K_3(\Phi)}{K_4(Zry)} \qquad \text{(A2)}$$

where

$K_4(Zry)=1$ Zircaloy-4 (A3-1)

$K_4(Zry)=1.305$ Zircaloy-2 (A3-2)

$$K_1(T)=1.17628\times10^{9}+4.54859\times10^{5}T$$
$$-3.28185\times10^{3}T^{2}+1.72752T^{3} \qquad T<750\ \text{K} \qquad \text{(A4-1)}$$

$$K_1(T)=2.522488\times10^{6}\exp\left(\frac{2.8500027\times10^{6}}{T^{2}}\right) \qquad 750\le T<1090\ \text{K} \qquad \text{(A4-2)}$$

$$K_1(T)=1.841376039\times10^{8}-1.4345448\times10^{5}T \qquad 1090\le T<1255\ \text{K} \qquad \text{(A4-3)}$$

$$K_1(T)=4.330\times10^{7}-6.685\times10^{4}T$$
$$+3.7579\times10^{1}T^{2}-7.33\times10^{-3}T^{3} \qquad 1255\le T\le2100\ \text{K} \qquad \text{(A4-4)}$$

$K_1(T)=1.0$ $2100\ \text{K}<T$ (A4-5)

$$K_2(CW)=0.546CW \qquad \text{(A5)}$$

$K_3(\Phi)=(-0.1464+1.464\times10^{-25}\Phi)f(CW,T)$ $\Phi<0.1\times10^{25}\ \text{m}^{-2}$ (A6-1a)

$$f(CW,T)=2.25\exp(-20CW)\times\min\left[1,\exp\left(\frac{T-550}{10}\right)\right] \qquad \text{(A6-1b)}$$

$K_3(\Phi)=2.928\times10^{-26}\Phi$ $0.1\times10^{25}\le\Phi<2\times10^{25}\ \text{m}^{-2}$ (A6-2)

$K_3(\Phi)=0.53236+2.6618\times10^{-27}\Phi$ $2\times10^{25}\le\Phi<7.5\times10^{25}\ \text{m}^{-2}$ (A6-3)

$K_3(\Phi)=0.731995$ $7.5\times10^{25}\ \text{m}^{-2}\le\Phi$ (A6-4)

The strain rate exponent:

$$m = 0.015 \qquad T < 750 \text{ K} \qquad \text{(A7-1)}$$

$$m = 7.458\times10^{-4}T - 0.544338 \qquad 750 \le T \le 800 \text{ K} \qquad \text{(A7-2)}$$

$$m = 3.24124\times10^{-4}T - 0.20701 \qquad 800 \text{ K} < T \qquad \text{(A7-3)}$$

The strain hardening exponent:

$$n = \frac{n_1(T)n_2(\Phi)}{n_3(Zry)} \qquad \text{(A8)}$$

where

$$n_3(Zry) = 1 \qquad \text{Zircaloy-4} \qquad \text{(A9-1)}$$

$$n_3(Zry) = 1.6 \qquad \text{Zircaloy-2} \qquad \text{(A9-1)}$$

$$n_1(T) = 0.11405 \qquad T < 419.4 \text{ K} \qquad \text{(A10-1)}$$

$$n_1(T) = -9.490\times10^{-2} + 1.165\times10^{-3}T - 1.992\times10^{-6}T^2 + 9.558\times10^{-10}T^3 \qquad 419.4 \le T < 1099.0722 \text{ K} \qquad \text{(A10-2)}$$

$$n_1(T) = -0.22655119 + 2.5\times10^{-4}T \qquad 1099.0722 \le T < 1600 \text{ K} \qquad \text{(A10-3)}$$

$$n_1(T) = 0.17344880 \qquad 1600 \text{ K} \le T \qquad \text{(A10-4)}$$

$$n_2(\Phi) = 1.321 + 0.48\times10^{-25}\Phi \qquad \Phi < 0.1\times10^{25} \text{ m}^{-2} \qquad \text{(A11-1)}$$

$$n_2(\Phi) = 1.369 + 0.096\times10^{-25}\Phi \qquad 0.1\times10^{25} \le \Phi < 2\times10^{25} \text{ m}^{-2} \qquad \text{(A11-2)}$$

$$n_2(\Phi) = 1.5435 + 0.008727\times10^{-25}\Phi \qquad 2\times10^{25} \le \Phi < 7.5\times10^{25} \text{ m}^{-2} \qquad \text{(A11-3)}$$

$$n_2(\Phi) = 1.608953 \qquad 7.5\times10^{25} \text{ m}^{-2} \le \Phi \qquad \text{(A11-4)}$$

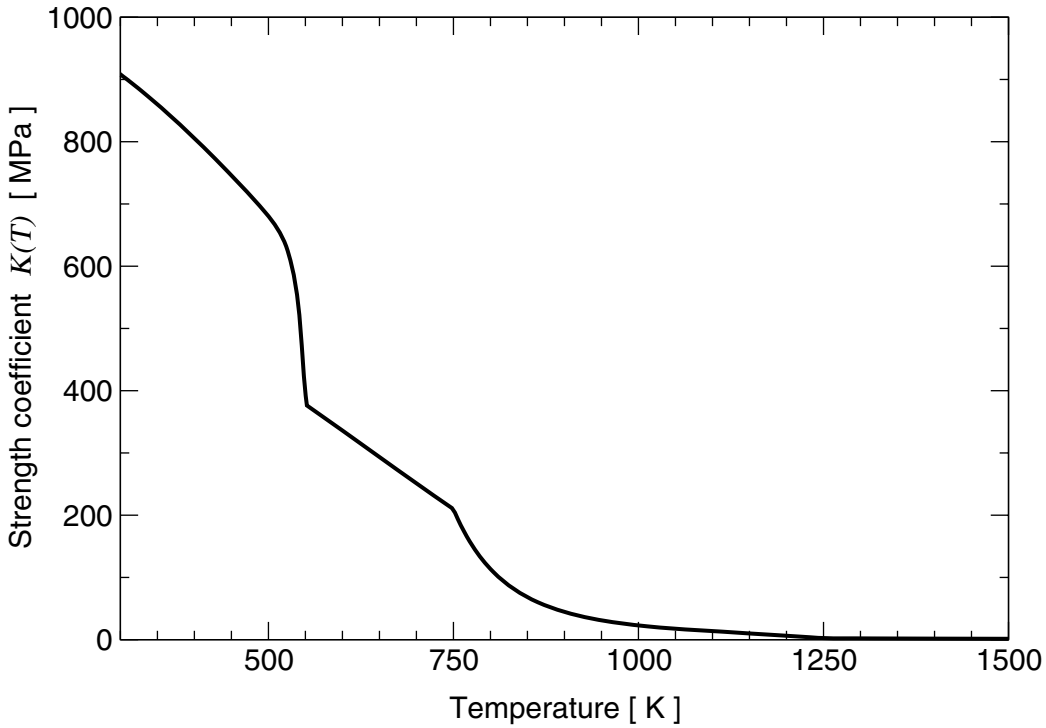

Figure A2: Strength coefficient K(T) according to eqs. (A4).

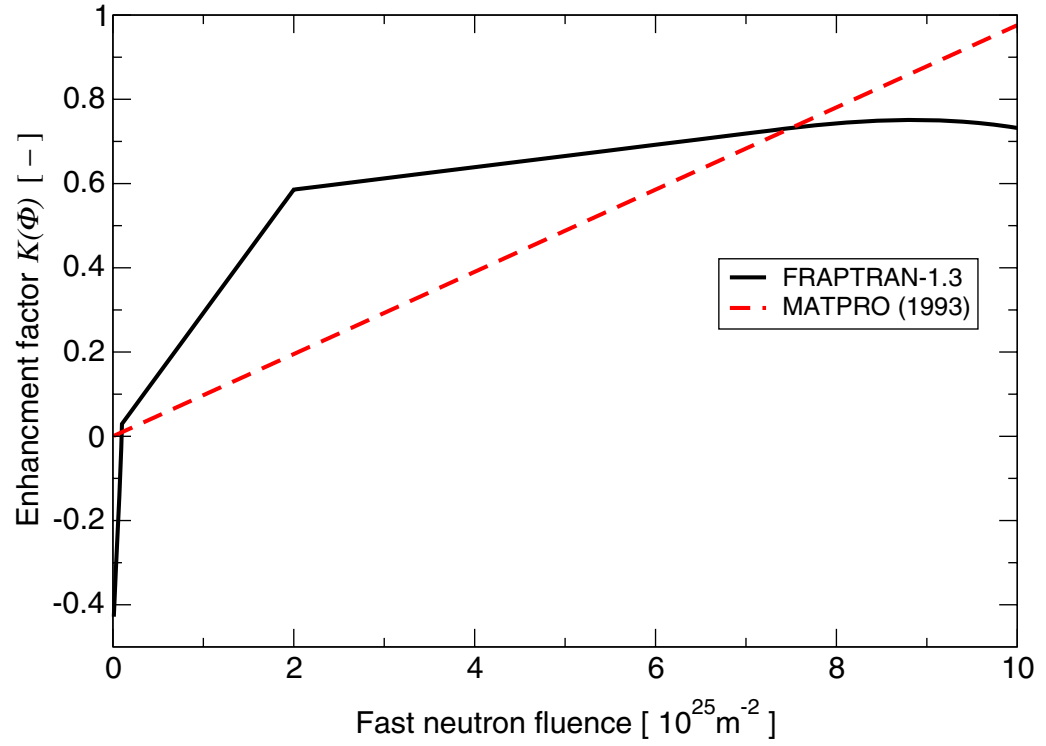

Figure A3: Enhancement factor K(Φ) in FRAPTRAN-1.3 according to eqs. (A6) and comparison with MATPRO (Allison et al., 1993).

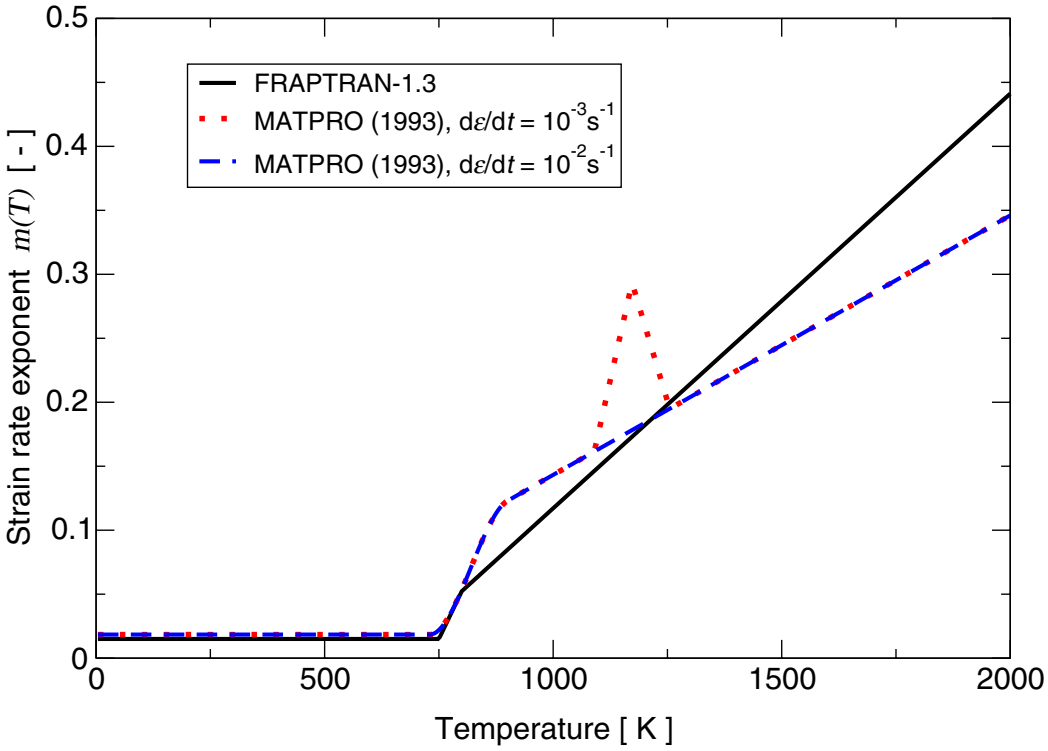

Figure A4: Strain rate coefficient m(T) in FRAPTRAN-1.3 according to eqs. (A7) compared with MATPRO (Allison et al., 1993). In MATPRO, the strain rate exponent is enhanced in (α+β) phase temperature range for strain rates exceeding 6.34×10^{-3} s^{-1}.

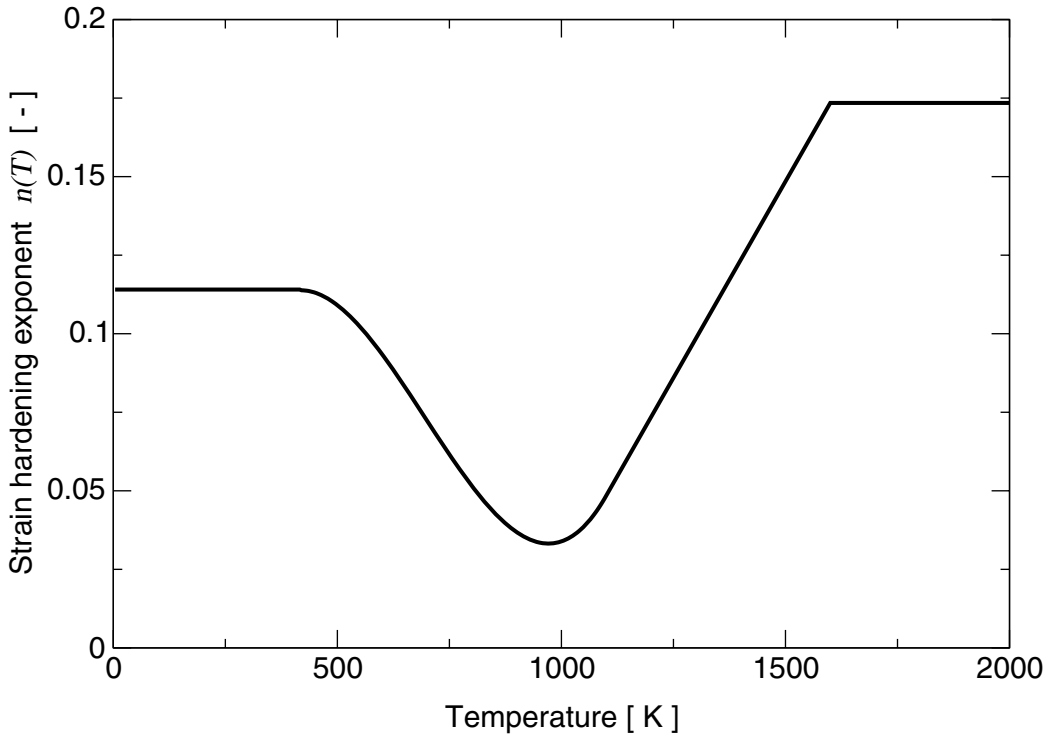

Figure A5: Strain hardening exponent n(T) according to eqs. (A10).

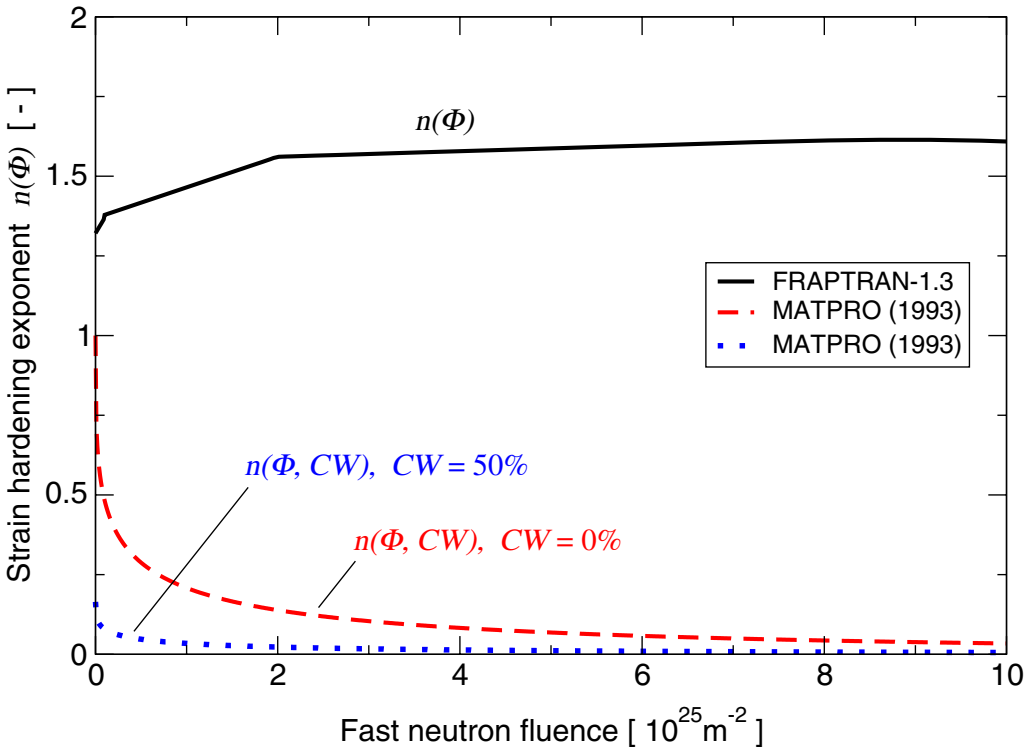

Figure A6: Strain hardening exponent n(Φ) in FRAPTAN-1.3 according to eqs. (A11) compared with MATPRO (Allison et al., 1993). In MATPRO, a dependency on cold work is included in the fluence factor of the strain hardening exponent.

Appendix B: FRAPTRAN-1.3 results of NRU MT-4 LOCA test

The MT-4 LOCA test was run as a sample case with FRAPTRAN-1.3 to illustrate some of the key results calculated by the code. The active length of the rod in the analysis is divided into 12 equally long axial segments. In the thermal calculations, the fuel and cladding are radially divided into 25 and 2 nodes, respectively. The axial power profile of the rod is plotted in figure B1. The coolant pressure is constant (0.276 MPa) in the case, whereas the coolant mass flow rate varies between 0 and 140 $kg/m^2/s$.

Rod burst is retrodicted to occur at about 60 s after initiation of the event which is slightly in excess of the average rupture time of 55 s measured in the test. The burst location coincides with the axial peak power position, i.e. in segment 8 at the axial elevation of 2.286 m. The occurrence of rod burst is seen in the plot of calculated rod internal pressure versus time as an abrupt decrease in the pressure, see figure B2. The maximum rod internal pressure (12.3 MPa) is attained just before the cladding instability strain is reached at about 30 s. At this point in time the calculation of the local deformations in axial segment 8 is switched on to be calculated by the ballooning model. The calculated cladding hoop strains (total and plastic) as a function of time are plotted in figure B3. The maximum calculated plastic hoop rupture strain is about 32.5% which is much less that the average hoop rupture strain of 72% obtained in the test. The variation of the clad-to-coolant heat transfer coefficient in the burst segment during the actual calculation is plotted in figure B4.

The calculated clad inner and outer surface oxide layer thicknesses in axial segment 8 are plotted in figure B5. We note that FRAPTRAN calculates double-sided oxide growth. The initial thickness at both surfaces prior to the test is 3 μm.

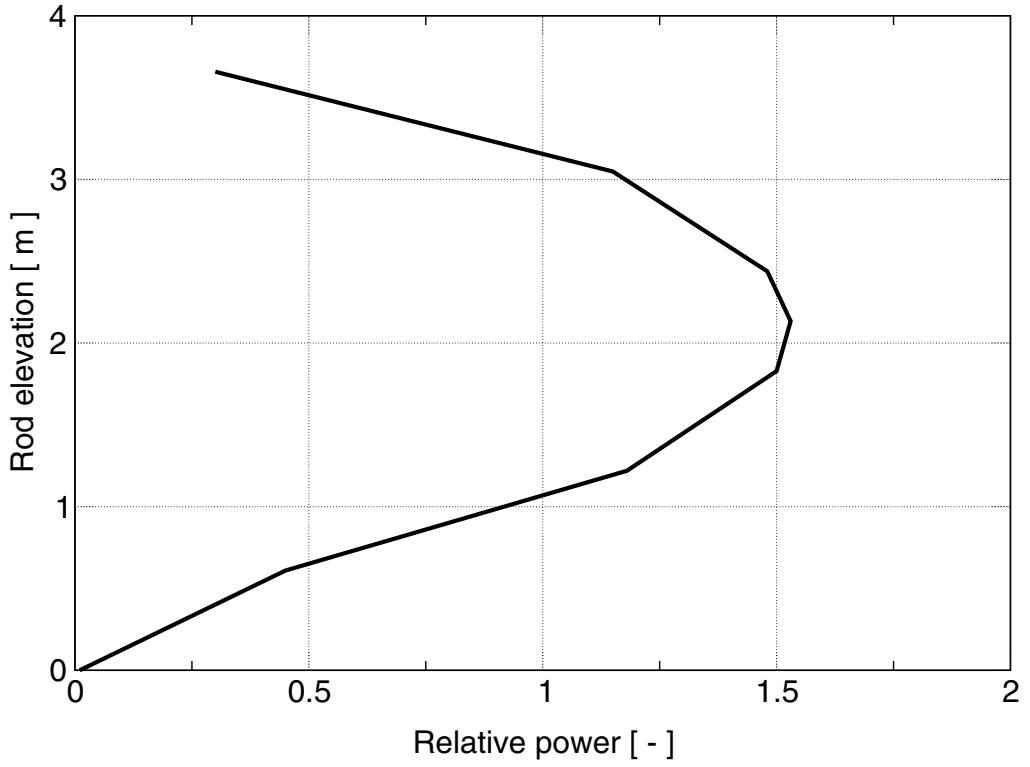

Figure B1: Axial power profile used in FRAPTRAN-1.3 for the MT-4 test case. From assessment database input file provided at www.pnl.gov/frapcon3.

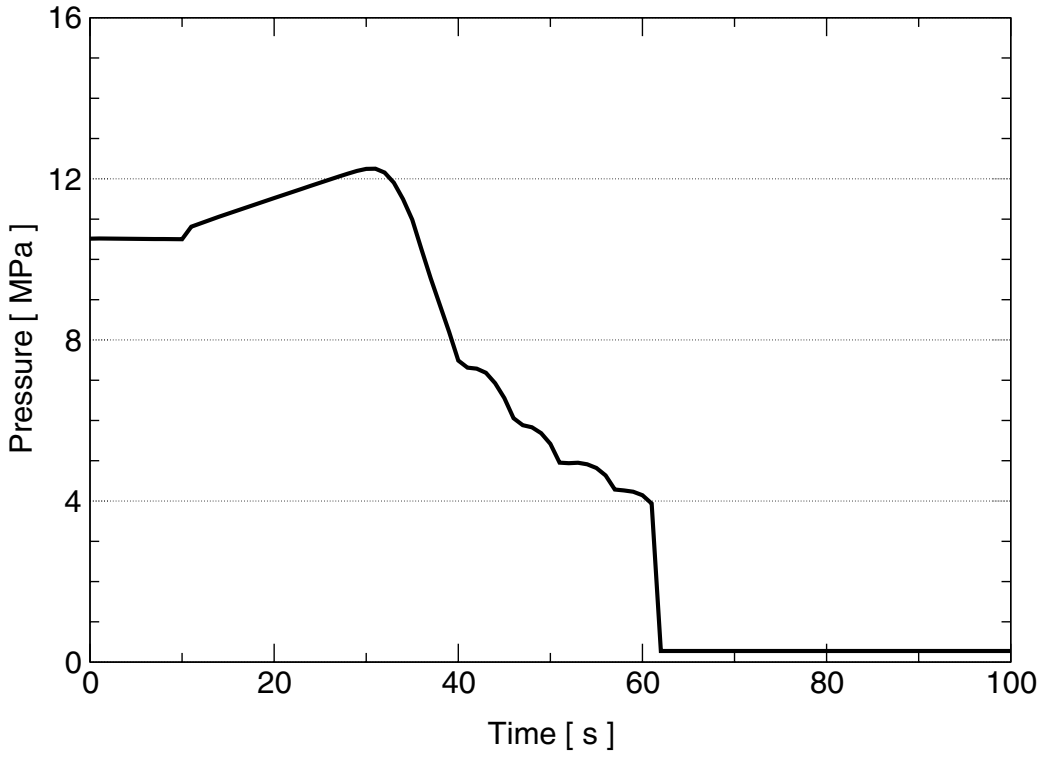

Figure B2: Calculated plenum gas pressure by FRAPTRAN-1.3, MT-4 test. Rod burst is retrodicted to occur at about 60 s after initiation of the LOCA test.

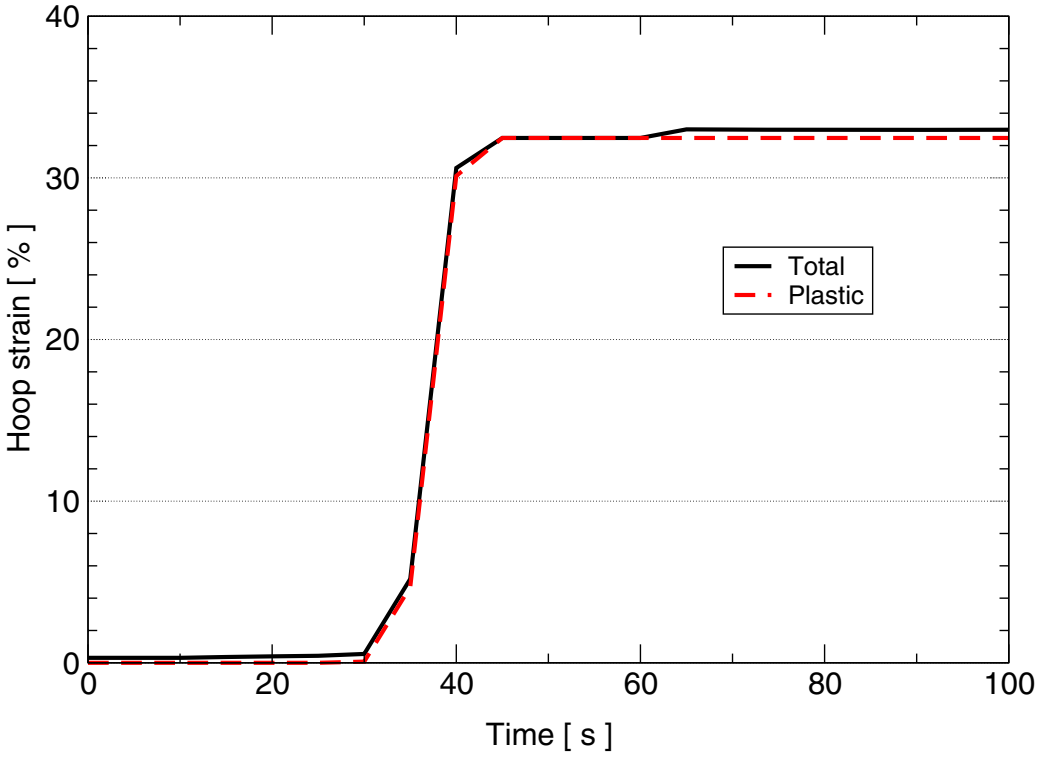

Figure B3: Calculated clad hoop strain in axial segment 8 by FRAPTRAN-1.3, MT-4 test.

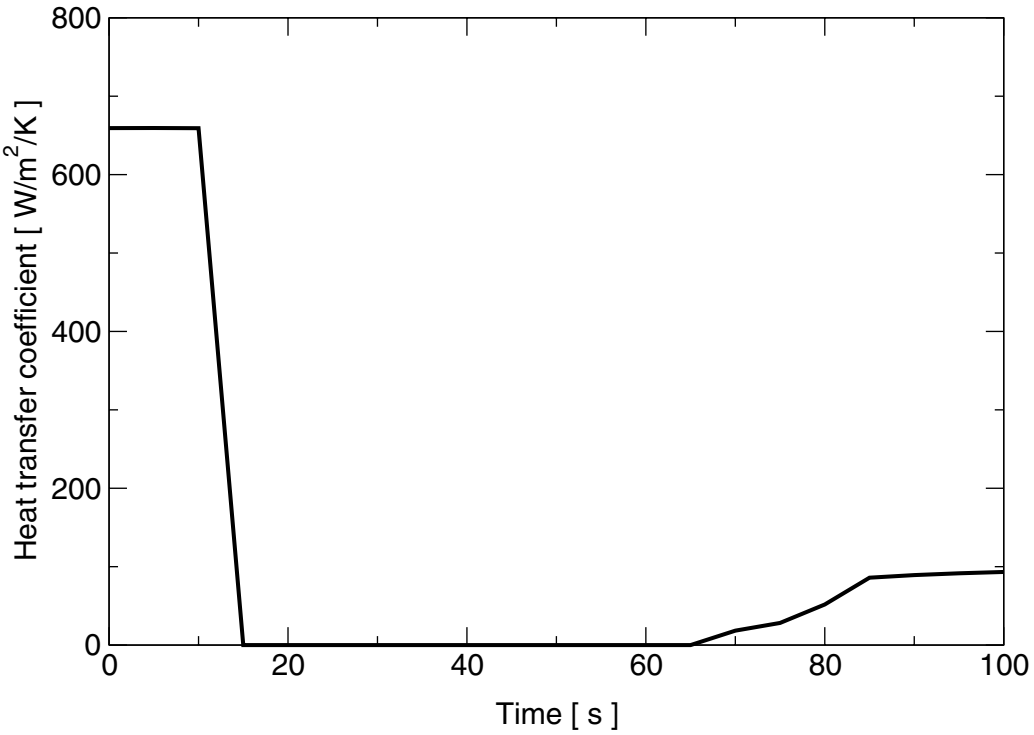

Figure B4: Clad-to-coolant heat transfer coefficient in axial segment 8 used in FRAPTRAN-1.3 analysis of the MT-4 test.

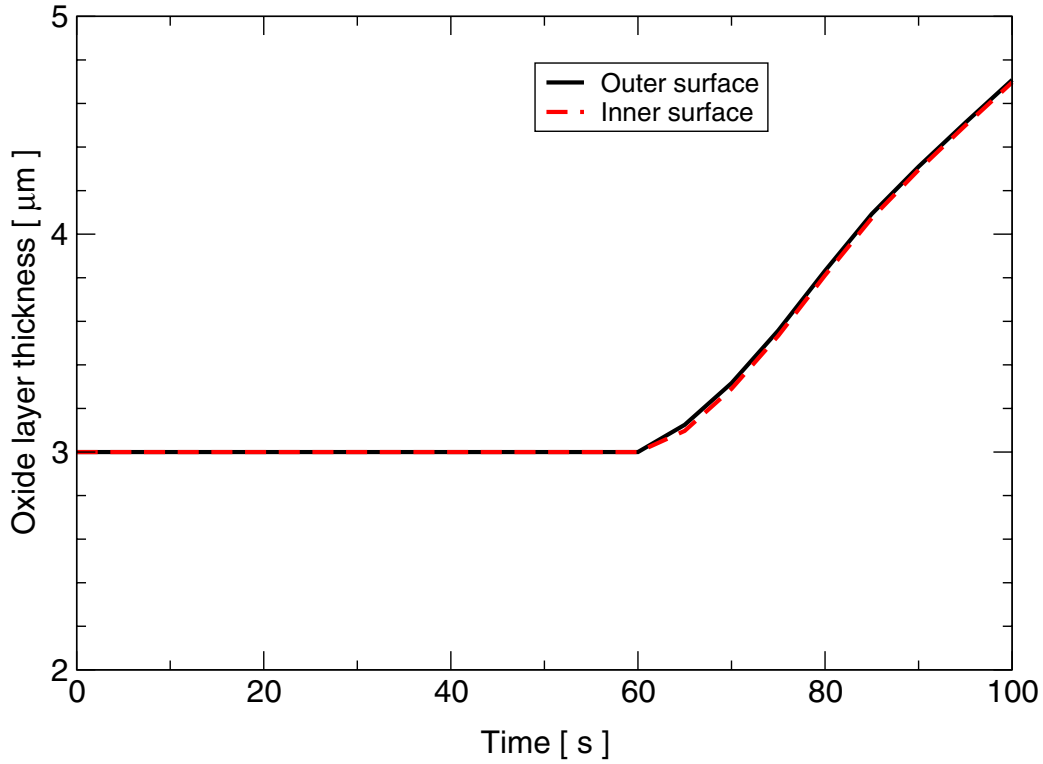

Figure B5: Calculated oxide layer thicknesses (at inner and outer tube surfaces) in axial segment 8 by FRAPTRAN-1.3, MT-4 LOCA test.

Appendix C: Selection of critical heat flux and film boiling correlations

The modelling options for selecting critical heat flux (CHF) and film boiling (FB) correlations for application in the coolant channel model of FRAPTRAN-1.3 are defined here. Seven options are available for critical heat flux calculation and five for determining the heat transfer coefficient under film boiling conditions.

The CHF and FB correlations together with the respective input option parameters, `jchf` and `jfb`, are shown in tables B1 and B2. Note that a change of the respective correlations, CHF and FB, are activated by assigning the parameters `chf` and `filmbo` to unity, e.g. a change of the default CHF correlation to the CE-1 correlation is achieved by setting `chf=1` and `jchf=4`.

`jchf`	**Critical heat flux correlation**	**Comment**
0	BW-2 with Barnett	
1	GE	
2	Savannah River	
3	Combination of W-3, Hsu-Beckner, modified Zuber	Default
4	CE-1	
5	LOFT	
6	RELAP4 Mod7	

Table B1: Critical heat flux correlations in FRAPTRAN-1.3. The change of a correlation (`jchf`≠3) is turned on by setting the parameter `chf=1`. See appendix D in Cunningham et al. (2001a) for references on the correlations.

`jfb`	**Film boiling correlation**	**Comment**
0	Groeneveld, cluster geometry form	
1	Groeneveld, open annulus geometry form	
2	Doughall-Rohsenow	
3	Condie-Bengtson	
4	Combination of Tong-Young and Condie-Bengtson	Default

Table B2: Film boiling correlations in FRAPTRAN-1.3. The change of a correlation (`jfb`≠4) is turned on by setting the parameter `filmbo=1`. See appendix D in Cunningham et al. (2001a) for references on the correlations.

www.ski.se

STATENS KÄRNKRAFTINSPEKTION
Swedish Nuclear Power Inspectorate

POST/POSTAL ADDRESS SE-106 58 Stockholm
BESÖK/OFFICE Klarabergsviadukten 90
TELEFON/TELEPHONE +46 (0)8 698 84 00
TELEFAX +46 (0)8 661 90 86
E-POST/E-MAIL ski@ski.se
WEBBPLATS/WEB SITE www.ski.se